ISTANBUL TECHNICAL UNIVERSITY ★ GRADUATE SCHOOL OF SCIENCE ENGINEERING AND TECHNOLOGY

AEROACOUSTIC ANALYSIS OF OPEN CAVITIES WITH ROUNDED EDGES

M.Sc. THESIS

Evren YENIGELEN

Department of Aeronautical and Astronautical Engineering

Aeronautical and Astronautical Engineering Programme

JUNE 2015

ISTANBUL TECHNICAL UNIVERSITY ★ GRADUATE SCHOOL OF SCIENCE ENGINEERING AND TECHNOLOGY

AEROACOUSTIC ANALYSIS OF OPEN CAVITIES WITH ROUNDED EDGES

M.Sc. THESIS

Evren YENIGELEN
(511131113)

Department of Aeronautical and Astronautical Engineering

Aeronautical and Astronautical Engineering Programme

Thesis Advisor: Prof. Dr. Metin Orhan KAYA

JUNE 2015

İSTANBUL TEKNİK ÜNİVERSİTESİ ★ FEN BİLİMLERİ ENSTİTÜSÜ

KÖŞELERİ YUVARLANMIŞ AÇIK KAVİTELERİN AEROAKUSTİK ANALİZLERİ

YÜKSEK LİSANS TEZİ

Evren YENIGELEN
(511131113)

Uçak ve Uzay Mühendisliği Anabilim Dalı

Uçak ve Uzay Mühendisliği Programı

Tez Danışmanı: Prof. Dr. Metin Orhan KAYA

HAZIRAN 2015

Evren YENIGELEN, a M.Sc. student of ITU Graduate School of Science Engineering and Technology 511131113 successfully defended the thesis entitled **"AEROACOUSTIC ANALYSIS OF OPEN CAVITIES WITH ROUNDED EDGES"**, which he prepared after fulfilling the requirements specified in the associated legis-lations, before the jury whose signatures are below.

Thesis Advisor :	**Prof. Dr. Metin Orhan KAYA** Istanbul Technical University	.....
Jury Members :	**Prof. Dr. Erol UZAL** Istanbul University	.....
	Assist. Prof. Özge ÖZDEMİR Istanbul Technical University	.....

Date of Submission : **04 May 2015**
Date of Defense : **04 Haziran 2015**

To my parents,

FOREWORD

First I would like to thank to my advisor Prof. Dr. Metin Orhan KAYA, who introduced me to aeroacoustics and Assist. Prof. Baha ZAFER who patiently taught me the details of CFD, coding and aeroacoustics, and helped me everytime throughout my graduate education.

I also want to thank to my dear friend Burak Tantay who helped me anytime without a doubt and used his immense coding talents to ease my way out this thesis. I am grateful to Kerem Aydemir for sharing his knowledge with me and to Göker Sunguroğlu who was a perfect companion while writing this thesis. Also I would like to thank my friend Kaan Yıldız for his continuous support and encouragement throughout this project.

But my strongest gratitude is to my parents. They have always supported me with all the choices I have made right or wrong and made me feel sure that they will be always there when I need them.

JUNE 2015 Evren YENIGELEN

TABLE OF CONTENTS

Page

FOREWORD ..... **ix**
TABLE OF CONTENTS ..... **xi**
ABBREVIATIONS ..... **xiii**
LIST OF FIGURES ..... **xv**
SUMMARY ..... **xvii**
ÖZET ..... **xix**
1. INTRODUCTION **1**
1.1 Purpose of Thesis 2
1.2 Overview 3
2. CAVITY FLOW **5**
2.1 Introduction 5
2.2 Oscillation Types Occur in Cavity Flows 6
2.3 Effects of the Cavity Geometry 7
2.4 Flow Features 8
2.5 Control of Cavity Noise 9
3. AEROACOUSTICS **11**
3.1 Introduction 11
3.2 Acoustic Analogies 11
3.2.1 Lighthill's Analogy 12
3.2.2 Ffowcs Williams and Hawkings' Equation 12
3.2.3 Curle's Equation and the Modifications Used 13
4. CFD INVESTIGATION **17**
4.1 Introduction 17
4.2 Cavity Geometries 17
4.3 Mesh Properties 19
4.4 Modelling Physics 21
4.4.1 Modelling flow and energy 21
4.4.2 Modelling turbulence 22
4.4.2.1 Introduction 22
4.4.2.2 Turbulence models 23
4.5 Boundary Conditions 25
5. RESULTS AND DISCUSSION **27**
5.1 CFD Results 27
5.1.1 Validation results 27
5.1.2 Unsteady flow field 28
5.1.3 Normalized pressure field 32
5.1.4 Aeroacoustic Results 35

6. CONCLUSIONS AND RECOMMENDATIONS 43
REFERENCES 45
CURRICULUM VITAE 47

ABBREVIATIONS

CFD	**:** Computational Fluid Dynamics
DNS	**:** Direct Numerical Simulation
LES	**:** Large Eddy Simulation
OASPL	**:** Overall Averaged Sound Pressure Level
PIV	**:** Particle Image Velocimetry
RANS	**:** Reynolds-Averaged Naiver-Stokes
SPL	**:** Sound Pressure Level
SST	**:** Shear Stress Transport

LIST OF FIGURES

Page

Figure 1.1 : Airframes as noise sources. 1
Figure 2.1 : Cavity flow (Lazar et al., 2008). 6
Figure 2.2 : Categorization of cavity oscillation types (Rockwell and Naudascher, 1978). 7
Figure 2.3 : Different cavity noise control methods (Franke and Carr, 1975). 10
Figure 4.1 : Case 1 – Validation case with no rounded edges. 18
Figure 4.2 : Case 2 – Rounded leading edge. 18
Figure 4.3 : Case 3 – Rounded trailing edge. 19
Figure 4.4 : Case 4 – Rounded leading and trailing edge. 19
Figure 4.5 : Mesh of the validation case. 20
Figure 4.6 : Turbulent flow. 22
Figure 4.7 : Boundary types. 25
Figure 5.1 : Velocity vectors with line integral convolution; Left: Streamlines from Parkhi(2009), Right: Case 1. 28
Figure 5.2 : Normalized streamwise velocity fields; Left: Parkhi(2009), Right: Case 1. 28
Figure 5.3 : Normalized vertical velocity fields; Left: Parkhi(2009), Right: Case 1. 28
Figure 5.4 : Comparison of velocity magnitudes of validation and leading edge cases. 29
Figure 5.5 : Comparison of velocity magnitudes of validation and trailing edge cases. 30
Figure 5.6 : Comparison of velocity magnitudes of validation and both edges cases. 31
Figure 5.7 : Comparison of normalized pressure distributions of all cases at physical time of 0.0005 s. 32
Figure 5.8 : Comparison of normalized pressure distributions of all cases at physical time of 0.001 s. 33
Figure 5.9 : Comparison of normalized pressure distributions of all cases at physical time of 0.005 s. 33
Figure 5.10 : Comparison of normalized pressure distributions of all cases at physical time of 0.01 s. 34
Figure 5.11 : Comparison of normalized pressure distributions of all cases at physical time of 0.015 s. 34
Figure 5.12 : Listener positions. 36
Figure 5.13 : Sound pressures at listeners 1,2,3. 37
Figure 5.14 : Sound pressures at listeners 4,5,6. 38
Figure 5.15 : Sound pressure levels at listeners 1,2,3. 39

Figure 5.16: Sound pressure levels at listeners 4,5,6. 40
Figure 5.17: Overall averaged sound pressure levels at all listeners..... 41

AERO ACOUSTIC ANALYSIS OF OPEN CAVITIES WITH ROUNDED EDGES

SUMMARY

The main goal of this thesis is to understand the effect of rounding the edges of a cavity on sound generated by the cavity flow. To achieve this goal, the first step is to understand the physics of the flow. Then understand the aeroacoustic analogies and select the appropriate one for the specific case. Then conduct an effective CFD analysis and with the obtained data calculate the noise generated by the cavity flow using aeroacoustic analogies.

A wide literature review of on cavity flow physics has been conducted and it is seen that the most important feature of the cavity flow is the self-sustained oscillations. There are 3 main types of oscillations: fluid dynamic, fluid resonant and fluid elastic oscillations. These have different characteristics and it is important to know it is possible to see several of them in the same flow. The first step to understand the noise generated by the cavity and control it is to understand these mechanism in detail.

Aeroacoustics is the main focus of this thesis. Aeroacoustics can be explained briefly as the sound generated aerodynamically, which is also the name of Sir Michael James Lighthill's important paper. This topic became an important area of research nowadays, as the outcomes can cause distinguishable effects on many applications. In aircrafts sound generation can cause discomfort to passengers and humans nearby the airfields. Reducing the sound emissions from these sources is the most important way to effective noise control. To achieve this important goal aeroacoustic analogies are used. In this thesis a Modified Curle's Analogy used, as it deals with static compact bodies.

To use this analogy, unsteady pressure data obtained from the walls of the cavity is required. To obtain this data, a CFD analysis by using a commercial tool should be conducted. In this tool, an unsteady analysis with the time step of 10^{-7} is conducted. The solver was an implicit unsteady solver with the turbulence model of RANS and realizable $k-\varepsilon$ model with two layer all $y+$ wall treatment.

As the solution domain, a cavity with the aspect ratio of 2 is selected. The length of the cavity is 0.3 m and the depth of it is 0.015 m. This is selected as a validation case and it is compared with a thesis that conducted a PIV analysis on a cavity with the same geometry. After the validation is confirmed, analyses with 3 different geometries are conducted. First of the geometry has a rounded leading edge with the radius of 3 mm. Second geometry has a rounded trailing edge with the same radius and the last geometry has both of its edges rounded with the same radius.

Pressure data obtained from the CFD analyses and fed in to our source code that uses the Modified Curle's Equation to calculate the sound generated by the cavity. This source code give sound pressures as output and they are fed into an FFT code to get sound pressure level (SPL) values. After that OASPL datas are calculated and the first

case is validated with the validation thesis. The next step is to conduct analyses with different geometries and investigate the effects of the rounded edges.

KÖŞELERİ YUVARLANMIŞ AÇIK KAVİTELERİN AEROAKUSTİK ANALİZLERİ

ÖZET

Aeroakustik konusu son 50 yıl içerisinde ortaya çıkmış ve araştırmaların gün geçtikçe ivme kazandığı bir çalışma alanıdır. İlk olarak askeri bir araştırma olarak, savaş uçaklarından bırakılan füzelerin üzerine gelen yüklerin doğru hesaplaması yapılması amacıyla bu konu üzerine odaklanılmıştır. Daha sonra konu genişlemiş, jet gürültüsü, yolcu uçaklarında, havaalanı yakınında ve yolcuları rahatsız eden gürültülerin oluşumu ve çeşitli bir çok alanda araştırmalar devam etmektedir. Bu çalışmalardan bir tanesi de kavitelerde oluşan gürültünün araştırılmasıdır. Bu araştırmalar dahilinde savaş uçaklarının füze bölmesinde, arabalarda sunroof ve pencerelerde oluşan ses gibi konular üzerinde incelemeler yapılmaktadır. Kavite akışı ve aeroakustiği basit bir geometriye sahip olmasına rağmen bir çok farklı akış fiziğini ve fenomenini barındırmaktadır.

Bu tezin asıl amacı, köşeleri yuvarlanmış kavitelerin kavite akışı sebebiyle oluşan gürültü üzerine etkisini incelemektir. Bu amaca erişebilmek amacıyla öncelikle kavite akışlarının fiziklerinin doğru ve detaylı bir şekilde anlaşılması gerekmektedir. Ayrıca aeroakustik analojilerin incelenmesi ve konuya uygun olanının seçilmesi ve gerekiyorsa düzenlenmesi gerekmektedir. Daha sonra bu akışların doğru bir şekilde çözülebilmesi ve gerekli değerlerin elde edilmesi gelir. Elde edilen bu verilerden aeroakustik analojiler kullanılarak ses basınçları ve nihayetinde ses değerleri hesaplanılabilir. Böylece farklı geometriler kullanılarak yapılan analizler sonucu, yuvarlanmış kavite köşelerinin oluşan gürültüye etkisi incelenebilir.

Kavite akışı geometrik olarak basit görünmesine rağmen oldukça farklı fiziksel özelliği içinde bulundurak bir akış tipidir. Bu akış oldukça değişkendir ve birçok mekanizmanın etkisi altında kalmaktadır. Detaylı bir literatür araştırması sonucu bu akışı etkileyen en önemli mekanizmanın oto-osilasyon olduğu görülmüştür. Bu mekanizmada, kavite hücum kenarından kopan vorteksler ve oluşturdukları ses dalgaları akış yönünde ilerleyerek firar kenarına çarpmakta ve oradan geri besleme yaparak bir sonraki kopacak olak vorteksleri etkilemektedir. Bu mekanizma farklı geometriler ve akış şartlarında değişik özelliklere sahip olmaktadırlar. Bu mekanizma özlleklierine göre 3 ana başlığa ayrılabilir. Bunlar akış dinamik, akış rezonant ve akış elastik olarak adlandırılabilirler. Bu mekanizmaların hepsinin ayrı ayrı özellikleri olmasıyla birlikte bazı akışlarda aynı anda görülebiliyor olmalarının bilinmesi gerekmektedir. Bu osilasyon mekanizmalarının iyi anlaşılması, bu sebeple oluşan sesin kontrolünün daha etkili bir şekilde yapılmasını sağlayacaktır. Bu kontrol sistemleri aktif ve pasif olarak ayrılmakta ve çok geniş bir araştırma ağını kapsamaktadır. Bu ağ içerisinden doğru olanı seçmek için akış fiziğinin doğru anlaşılmış ve yeterli araştırmanın yapılmış olması gerekmektedir. Bu tezde pasif bir kontrol yöntemi olan geometri kenarlarının yuvarlatılması incelenecektir.

Diğer detaylı bir şekilde anlaşılması gereken konu ise aeroakustik analojilerdir. Ses bir akış alanındaki düzensizlikler olarak adlandırılabilir. Basınç ve mekanda olan bu değişiklikler akıştan dalga biçimde enerji kaçışına sebep olmaktadır. Bu enerji akışın kendisinin enerjisine göre oldukça düşüktür, bu da zaten çözülmesi zor olan bir problemin çözümünü daha zor hale getirmiştir. Aeroakustikte basit ve efektif bir analitik sonucun elde edilmesi hakkında umut verici bir gelişme gözükmemektedir. Bu sebeple daha çok nümerik çözümler üzerinde çalışmalar yapılmıştır. Bu çözümlerden ilki Lighthill tarafında yapılmıştır ve aeroakustik analoji ismi verilmiştir. Bu analojide genel Navier-Stokes denklemlerinde düzenlemeler ve benzetmeler yapılarak, akış tarafından oluşturulan sesin tahmini yapılabilmektedir. Bu çalışmadan sonra değişik ve farklı yönleri ele alan çalışmalar yapılmıştır. Bu tezde Curle'ün analojisi kullanılacaktır. Çünkü bu analoji Lighthill'in aksine katı yüzeylerin varlığını da işin içine katmaktadır. Bu analojinin üzerinde biraz basitleştirmeler yapılmış ve nümerik olarak kod içine basit bir şekilde aktarılabilecek bir versiyonu üzerinde yoğunlaşılmıştır. Analoji detaylı olarak incelenmiş ve yapılan basitleştirmelerin sebepleri ve doğruluğu tartışılmıştır.

Daha sonra bu kodun içerisine beslenecek olan kavite üzerindeki zamana bağlı basınç değerlerini elde etmek amacıyla bir Hesaplamalı Akışkanlar Dinamiği (HAD) analizi yapılmıştır. Bu analiz zamana bağlı olarak yapılmış ve zaman adımı olarak 10^{-7} kullanılmıştır. Analiz implicit bir çözücü kullanmaktadır ve türbülans modeli olarak RANS(Reynolds Averaged Navier-Stokes) ve "All $y+$ treatment" ile birlikte "$k-\varepsilon$" modeli kullanmaktadır. RANS modeli Navier-Stokes denklemlerinin zamanda ortalamasını alarak çözümlemeler yapmaktadır. Burada ortalama değerler ve bozuntularla ayrı ayrı ilgilenilmektedir. $k-\varepsilon$ modelindeyse viskozite k ve ε olmak üzere 2 denklem üzerinden hesaplanarak modelleme yapılmıştır. Burada çözüm alanının düzgün oluşturulması da çok önemlidir. Kavitenin içine, hücum ve firar kenarlarının etraflarına oldukça yoğun bir çözüm alanı uygulanarak, zamanla değişen düzensiz akışın doğru bir şekilde saptanması ve incelenmesi sağlanmaktadır. Bunun için sınrı tabakaya uygulanan çözüm alanına ve çözüm elemanları arasındaki geçişe dikkat edilmiştir. Sistemin doğruluğu kanıtlandıktan sonra hesaplama zamanını ve maliyetini azaltmak amacıyla çözüm alanının belli bölgelerinde düzeltmelere gidilebilir. Ancak düzeltme yapılan bu bölgeler dikkatle seçilmeli ve düzeltmeler akışın karakteristiğine etki etmeyecek şekilde yapılmalıdır.

CFD analizi için uzunluk-derinlik oranı 2 olan bir kavite kullanılmıştır. Kavitenin uzunluğu 0.3 m derinliği ise 0.15 m'dir. İlk analizde kavitenin kenarlarına bir yuvarlatma uygulanmamıştır ve bu analizin sonuçları aynı geometriyi ve fiziksel koşulları kullanarak PIV verileriyle analiz yapılmış olan bir tezle karşılaştırılmıştır. Karşılaştırma sonrası hız vektörlerinin ve basınç alanlarının oldukça yakın olduğu görülmüştür. Bu analizden kavitenin duvarları üzerinden zamana bağlı basınç değerleri depolanmış ve kendi aeroakustik kodumuzun içine beslenmiştir.

Bu kod belirtilen analojiyi kullanarak, farklı dinleyici noktalarında ses basıncı hesaplayabilmektedir. Kod içerisinde 9 farklı dinleyici noktasında ses basıncı değerleri hesaplanmıştır. Bu değerler bir FFT koduna girilerek ses basıncı düzeyleri elde edilmiştir. Daha sonra ortalama ses basıncı değerleri hesaplanarak validasyon tezi ile karşılaştırılmıştır. Bunun sonucunda da oldukça yakın değerler ortaya çıktığı görülmüştür.

Bundan sonraki hücum, firar ve her iki köşesinin yuvarlatılmış olduğu 3 farklı geometri öncelikle CFD programında çözdürülecek, daha sonra da elde edilen değerlerle ses basıncı düzeylerinde ne gibi bir etki yarattığı incelenecektir.

1. INTRODUCTION

Aeroacoustics can be explained briefly as the sound generated aerodynamically, which is also the name of Sir Michael James Lighthill's important paper. This topic became an important area of research nowadays, as the outcomes can cause distinguishable effects on many applications. In aircrafts sound generation can cause discomfort to passengers and humans nearby the airfields. The most obvious noise sources in aircrafts are jet-engines and the researches on this issue continue rapidly.

Another significant noise source is the airframe that can be seen in Figure 1.1, which includes, weapon bays, landing gears and fuel vents etc. Reducing the sound emissions from these sources is the most important way of effective noise control. This control system can be passive or active. The research done by scholars and engineers are focused on locating the significant sources of sound and reducing the intensity and loudness of the sound by various control options. One of the important type of airframe noises if cavity noise. Noise generating cavities like landing gears, fuel vents, windows of ground vehicles, sunroofs, car handles and any possible space that has the shape of a cavity that under the influence of fluid flows are in the range of cavity aeroacoustics researches. These noise generated from these cavities have effects on both ecology and in some cases mechanical stability of structures.

Figure 1.1: Airframes as noise sources.

One of the important type of airframe noises if cavity noise. Noise generating cavities like landing gears, fuel vents, windows of ground vehicles, sunroofs, car handles and any possible space that has the shape of a cavity that under the influence of fluid

flows are in the range of cavity aeroacoustics researches. These noise generated from these cavities have effects on both ecology and in some cases mechanical stability of structures.

For a start, modeling and working on a simple rectangular cavity, is an important step on understanding the nature of noise generated from cavities, these kinds of components like door handles, weapon bays and wheel wells. Depending the size and shape of the cavity and flow conditions the aeroacoustic outcomes of such geometries become sufficiently difficult to deal with as a starting point, and investigating cases with different specifications gives a good idea of how to make an efficient noise control. This investigation includes both the difficulties of correctly modeling the flow mechanism, numerically and/or experimentally, and the prediction of sound generation mechanism of the flow data gathered from the first step.

The first step of formulating the sound generated by fluid flow was the work of Lighthill in 1952. He rearranged the Navier-Stokes equations and suggested an acoustic analogy that can be used to calculate the noise produced by a fluid motion in an ambient environment. This study was a real success and opened new study paths for scholars and engineers working on this area. What Lighthill started on 1952 is continued by many researchers and specific analogies for different cases are developed. As a matter of fact, these analogies handle the flow and acoustic phenomena separately, so this thesis will include two parts of predicting the noise generated: computational fluid dynamics and computational aeroacoustics.

1.1 Purpose of Thesis

Purpose of this thesis is to investigate the flow physics and aeroacoustic results of an open cavity. To achieve this a commercial CFD tool and our own code for sound prediction will be used. After the validation of our results, investigation of the aeroacoustic results of rounding the edges of an open cavity will be conducted. In all of the analyses, all of the properties including boundary conditions and flow properties will be same and only the cavity geometry will change. The effects of rounding the leading edge, trailing edge and both edges will be investigated. With these investigations, the aim is to understand the effects of this specific geometry change

on flow physics and sound generated, and absolutely find a way to reduce the noise generation in open cavity flows.

1.2 Overview

Overall, this thesis will include research about cavity flow physics, aeroacoustic analogy and their implementation to cavity flow, CFD investigations on different open cavity geometries, and both CFD and aeroacoustic analyses results.

Chapter 1 gives an overall summary of this work and the focus it is dealing with with an introduction, purpose and an overview.

Chapter 2 deals with the details of cavity flow, what are the important properties, distinct mechanisms, results of changing the features and how to control this flow.

Chapter 3 gives detailed information about noise, aeroacoustics and the aeroacoustic analogy used in this thesis.

In Chapter 5, the properties of the CFD investigations are given, including the cavity geometries, mesh properties, flow physics and boundary conditions.

In Chapter 6, results of the CFD and aeroacoustic analyses are given and discussions about them are conducted.

Chapter 7 is a conclusion of this work and there are some suggestions about the future works that may be conducted to improve this work.

2. CAVITY FLOW

2.1 Introduction

The flow over the cavities which is a special area of aeroacoustics is an interesting area as Moon et al. (2003) stated as the tonal noise is generated by the periodically oscillating flow over the cavity, and a feedback mechanism is the reason of the unsteady nature of the flow. The main physics of the cavity flow is depicted in Figure 2.1. Self-sustained oscillations can be counted as one of the most important sources of the noise generated by the flow over a cavity. This important source has been an investigation focus for a long time, as stated by Colonius (2001) the underlying physical mechanisms of self-sustained oscillations are not yet clear enough. There are two main modes that trigger the self-sustained oscillations which are shear layer mode and relatively poor understood wake mode that was observed by Gharib and Roshko (1987). In the shear layer mode the shear layer spanning the leading edge of the cavity causes small disturbances which grow in magnitude by Kelvin-Helmholtz instability. The interaction of these disturbances with the trailing edge causes unstable flow features that effects the upstream flow which effects the shear layer as a feedback. In shear layer mode the shear layer stagnates at the trailing wall, but in wake mode the stagnation of the flow occurs before the trailing wall which means that the shear layer reattached to the base of the cavity. Gharib and Roshko (1987) identified the flow similar to a bluffbody wake which gave the mode of its name. In this mode the self-oscillations in the shear layer mode disappears and the flow becomes unstable on a large scale. Also they noted that the drag caused by the cavity increased significantly. As the wake mode will not play a role in this work, it will not be investigated more in detail. However, investigating the modes of the oscillations will be useful.

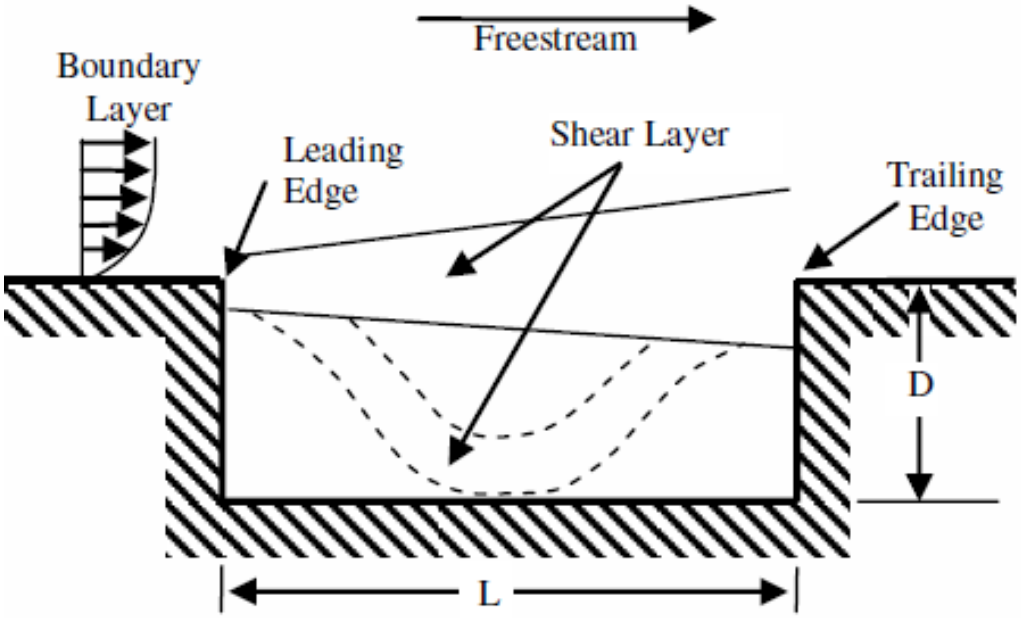

Figure 2.1: Cavity flow (Lazar et al., 2008).

2.2 Oscillation Types Occur in Cavity Flows

The oscillations were classified by Rockwell and Naudascher (1978) in three main topics; fluid-dynamic, fluid-resonant and fluid-elastic, which can be seen in Figure 2.2.

Fluid-dynamic oscillations are related to the acoustic feedback. It is described by Rossiter (1964) as a vortex shedding formed at the cavity leading edge colliding with the downstream wall and resulting an acoustic wave that travels back upstream and causing disturbance to the new vortexes forming at the leading edge. Rockwell and Naudascher (1978) stated the amplification of unstable disturbances in the cavity shear layer are the main reason for the stimulation of fluid-dynamic oscillations. And the main reason of the amplification is the presence of the downstream edge. It is added in the work that the two important aspects that should be focused are the amplification conditions of shear layer instability and the feedback condition. The disturbances in the cavity edge feed the shear layer instabilities and the amplification grows with the aid of this feedback.

Fluid resonant oscillations are classified by Rockwell and Naudascher (1978) as the self-sustaining cavity oscillations which are strongly coupled with resonant wave effects within the cavity. In this case, the acoustic wavelength becomes the same order

of magnitude or smaller than one of the cavity dimensions. This cavity oscillation occurs at certain values of wavelengths which is the explanation of standing waves in the cavity.

Fluid-elastic cavity oscillations can be described as the cavity itself forced in to large displacements which becomes a feedback element on the shear-layer perturbations. The elastic displacement of the wall becomes an energy source for the flow which couples with the structural modes of the cavity.

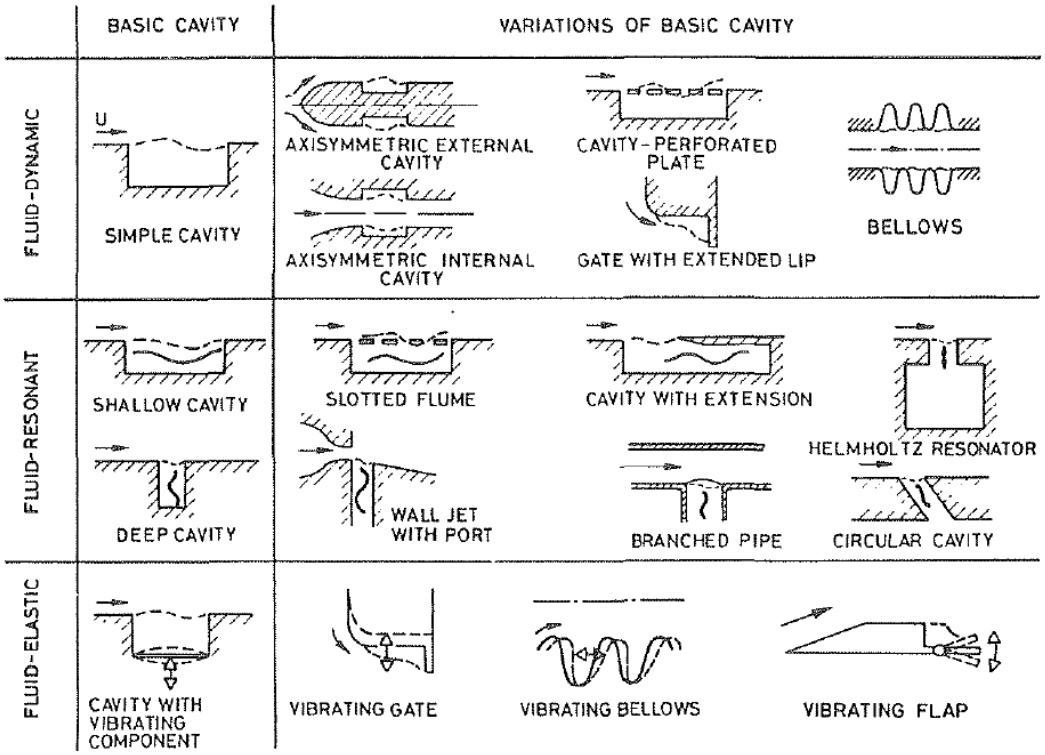

Figure 2.2: Categorization of cavity oscillation types (Rockwell and Naudascher, 1978).

2.3 Effects of the Cavity Geometry

It is useful to discuss the effects of the $\frac{L}{D}$ ratio and the 2D/3D effects of the cavities. To describe if the cavity is open, transitional or closed and shallow or deep, $\frac{L}{D}$ ratio is the variable to look on. Sarohia (1975) described that the cavities with aspect ratios larger than 1 are shallow cavities and the cavities with aspect ratios smaller than 1 are deep cavities. Though Rossiter (1964) claims that the value describes the shallowness or deepness is 4. There is the same disagreement on cavities being open or closed. To describe a cavity being open or closed it is better to look to the streamlines. In open cavities flow separates at the upstream of the cavity and reaches stagnation

point at the downstream of the cavity. In closed cavities the flow separates from the leading edge, reaches impingement and exit shocks at the bottom of the cavity and stagnates at the trailing edge of the cavity. In the manner of $\frac{L}{D}$ open cavities can be considered as the cavities that have aspect ratios lower then 9, transitional cavities have aspect ratios between 9 and 13 and cavities with aspect ratios higher than 13 can be considered as closed. Better to describe open cavities are the cavities that the separation of the boundary layer occurs at the leading edge and reattaches at the trailing edge. In open cavities shear-layer mode appears and the characteristic of this phenomenon is shear-layer reattachment at the downstream wall. When the separation appears at the base of the cavity that cavity is considered as a closed cavity. Back in if a cavity is shallow or deep, open cavities with $\frac{L}{D} > 1$ can be considered as shallow and cavities $\frac{L}{D} < 1$ can be considered deep. Deep cavities results in resonant oscillations that occurs in specific flow conditions which assures the natural acoustic depth modes of the cavities. In the studies of Karamcheti (1956), it is shown that no sound emission occurs below a certain cavity length or under a certain Mach number. The forming of sound emissions are dependent as well as on flow properties that will be explained in the next section.

It is well known that the cavity flow in reality is highly unsteady and three-dimensional. It is important to decide if it is accurate to analyze a cavity in 2D without ignoring important 3D effects. The work of Maull and East (1963) shows that the spanwise separation at the base of the cavity becomes an asymmetric wave-like pattern rather than a straight line. It is important to decide which part of the acoustic field is concerned as Ahuja and Mendoza (1995) showed that in far-field acoustic calculations, with cavities of $\frac{L}{W} < 1$ flow can be considered as 2D. However, the cavities with $\frac{L}{W} > 1$, the flow field appears to be 3D.

2.4 Flow Features

Flow properties highly effect the physics of cavity flows. In this thesis, open cavities which are mostly dominated by feedback mechanisms will be investigated. In these type of cavities with increasing Mach number the noise levels get louder in every part of the spectrum. The nonlinear effects in the flow have low effects in higher Mach numbers and the presence of higher-order harmonics can be observed. Transonic and

supersonic speeds are not in the investigation focus of this thesis. The oscillations are highly effected by the shear layer ability to roll up in to vortices. The boundary layer separating from the leading edge of the cavity should have certain properties to be able to form vortices. This is mostly dependent on the momentum thickness of this boundary layer. As stated by Sarohia (1976) there is a minimum cavity length that the laminar shear layer is not able to roll up. This mechanism of vortex forming is dependent as well as on the Reynolds number. Gloerfelt (2009) stated that the influence of Kevin-Helmholtz instability on the shear layer roll ups becomes insignificant in high Reynolds numbers ($Re_L > 106$) and therefore the importance of the thickness of the incoming boundary layer diminishes. Also he discusses that in moderate ranges of Reynolds numbers, large-scale vortices formed by a number of small-scales vortices can be examined. He summarized it as with high Renolds numbers cavity flows can be explained with two phenomena of broadband small-scales typical of turbulent shear layers, and discrete self-sustained oscillations due to a feedback phenomenon or a cavity resonance. The self-sustained oscillations are examined in many stable states of different modes in high Reynolds number cavity flows as the dominant structures of small scales are in different sizes.

2.5 Control of Cavity Noise

There are many past efforts to control the oscillations in the cavity, thus reducing the radiated noise levels. These massive varieties of control strategies, which are the evidence of different mechanisms that drives the cavity flow, are classified by Gloerfelt (2009) in 3 main topics: Passive control, Active Control and High frequency control. It would be a different work to examine all these strategies, so the strategy that is the focus of this current work will be investigated in detail. As Sarohia (1977) states in the third conclusion of the work, “The radiated cavity flow noise from shallow cavities is due to interaction of the violently oscillating shear layer with the downstream cavity corner.” Based on this conclusion, Pereira and Sousa (1993) made experiments with cavities that have different downstream wall geometries, focusing on circulating the edge of the trailing edge to examine the influence of impingement edge on cavity flow oscillations. They examined attenuation of the fluctuation peak magnitudes for the nose-shape impingement edge. Also, Rockwell and Naudascher (1978) referenced the

works of Ethembabaoglu which includes many different cavity geometries including ramps, spoilers, and radii on leading and trailing edge, which are categorized in Figure 2.3. He stated that ramps and radii on the trailing edge decreased the oscillations most effectively. He also added that the work of Franke and Carr (1975) shows that using ramps on both edges of the cavity has significant effects on attenuation of shallow cavity oscillations. In this thesis, effects of rounded cavity edges on sound generated aerodynamically will be investigated.

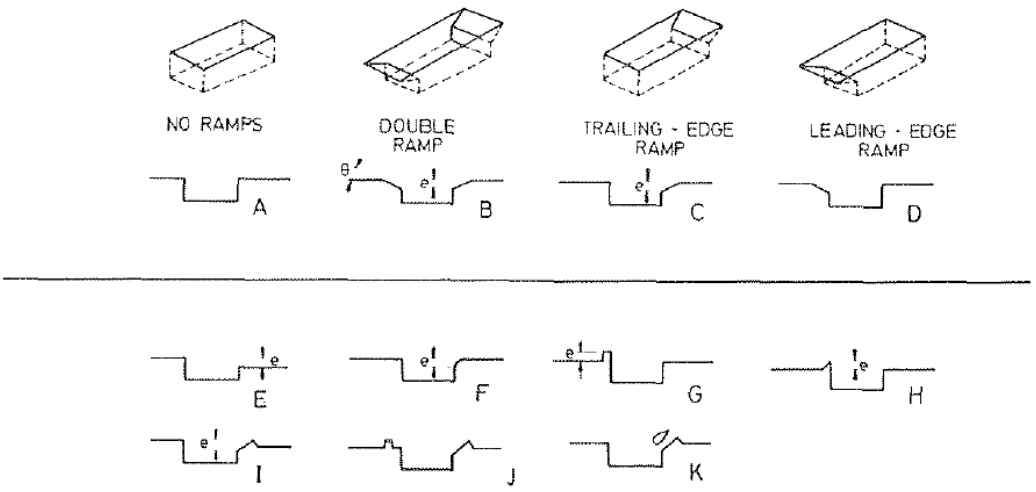

Figure 2.3: Different cavity noise control methods (Franke and Carr, 1975).

3. AEROACOUSTICS

3.1 Introduction

Sound production of fluid flows is very complicated and difficult to predict, as the governing equations the so-called Navier-Stokes equations are nonlinear. The energy of sound production is very small compared to the rest of the flow energy, which makes it more difficult to predict, and it gets harder and harder when the flow is in free space with low subsonic speeds. Nevertheless, some approximate solutions can be obtained by using the fact that sound field is a small perturbation of the flow (Hirschberg and Rienstra, 2004).

3.2 Acoustic Analogies

Aeroacoustics provide those approximate solutions by identifying the source of sound the difference between the actual flow and the reference flow, which means the perturbations in the flow. This is called an acoustic analogy and it is first introduced by Lighthill (1952). Selecting different variables in aeroacoustics leads to different reference flows and hence to different analogies. It is interesting to see that the same basic equations of fluid dynamics leads to different analogies by using different reformulations, but it is the essence of the analogy being an approximation. Moving on, although Lighthill‘s analogy is very general with no simplifications and the solution gathered from is exact, it is mostly useful for magnitude estimations, not for predicting sound by numerical simulations. Also, this analogy is solved for only free flow and does not include the effects of solid boundaries. Therefore, there have been different efforts to get analogies that are more efficient for numerical simulations for different applications. This thesis will focus on Curle‘s equation which includes the effects of stationary solid boundaries in his analogy.

3.2.1 Lighthill's Analogy

By re-arranging the Navier-Stokes equations of a compressible fluid, into an inhomogeneous differential wave equation with no simplifications, Lighthill (1952) became the pioneer of the field of aeroacoustic. By taking the time derivative of continuity equation and subtracting the divergence of momentum equation without considering external forces the equation below can be obtained:

$$\frac{\partial^2 \rho}{\partial t^2} - \frac{\partial^2 \rho u_i u_j}{\partial x_i x_j} = \frac{\partial^2 \rho}{\partial x^2} - \frac{\partial^2 \tau_{ij}}{\partial x_i \partial x_j} \tag{3.1}$$

Lighthill's derivation makes the connection between fluid mechanics and acoustics, and defines the true nature of sound sources in a turbulent flow. By adding $-a_\infty^2 \frac{\partial^2 \rho}{\partial x_i^2}$ to both sides of the equation above Lighthill's equation can be obtained:

$$\frac{\partial^2 \rho}{\partial t^2} - a_\infty^2 \frac{\partial^2 \rho}{\partial x_i^2} = \frac{\partial^2 T_{ij}}{\partial x_i \partial x_j} \tag{3.2}$$

where,

$$T_i j = \rho u_i u_j - \tau_{ij} + (p - a_\infty^2 \rho)\delta_{ij} \tag{3.3}$$

which is called Lighthill's stress tensor.

3.2.2 Ffowcs Williams and Hawkings' Equation

Ffowcs Williams and Hawkings (1969) extended the equation by taking account of the solid boundaries. The solid surfaces can have different effects on the sound generation as being sources of sound, or reflecting and diffracting the radiation sound which may change the radiation characteristics of the flow. Curle's work was former to Ffowcs Williams and Hawkings' but as the later one includes more physics in it, it is given before.

Ffowcs Williams and Hawkings used the same methodology with Lighthill but, added the source terms accounting the solid boundaries. After several mathematical arrangements the final equation yields as:

$$\begin{aligned}\rho(x,t)-\rho_0 =& \frac{1}{4\pi a_\infty^2}\frac{\partial^2}{\partial x_i \partial x_j}\int_V \frac{T_{ij}'^*}{r\left(1-\frac{l_j v_j}{a_\infty}\right)}dV(y^*) \\ &- \frac{1}{4\pi a_\infty^2}\frac{\partial}{\partial x_i}\int_S \frac{F_i^*}{r\left(1-\frac{l_j v_j}{a_\infty}\right)}dS(y^*) \\ &+ \frac{1}{4\pi a_\infty^2}\frac{\partial}{\partial t}\int_S \frac{Q^*}{r\left(1-\frac{l_j v_j}{a_\infty}\right)}dS(y^*)\end{aligned} \tag{3.4}$$

With the surface velocity v_i is constant, the source terms can be given as:

$$\begin{aligned}T_{ij}'^* &= \rho\left(u_i^*+v_i\right)\left(u_j^*+v_j\right)-\tau_{ij}^*+\left(p-a_\infty^2(\rho-\rho_\infty)\right)\delta_{ij} \\ F_i^* &= \left(\rho\left(u_i^*+v_i\right)u_j^*+p\delta_{ij}-\tau_{ij}^*\right)n_j \\ Q^* &= \left(\rho_\infty v_i+\rho u_i^*\right)n_i\end{aligned} \tag{3.5}$$

$T_{ij}'^*$ is formed by the fluctuating stresses in the fluid and represents the quadrupole sources. F_i^* represents the dipole sources due to fluctuating sources on the surface. Q^* is the monopole sources which is comprised by the fluctuating mass fluxes through the surface. It is important to state that in specific conditions Ffowcs Williams and Hawkings' equation and Curle's equation gives the same equation. u_i^* becomes 0 for impermeable surfaces so the dipole sources reduce to $F_i^* = (p\delta_{ij}-\tau'_{ij}*)n_j$ and monopole sources to $Q=\rho_\infty v_i n_i$. And when the surfaces are stationary as in Curle's equation monopole term dissapears.

3.2.3 Curle's Equation and the Modifications Used

As stated before, Curle's equation is the first equation that takes account of the presence of solid boundaries. In Curles's equation the velocity on surface is zero. The final equation of Curle can be given as:

$$\rho(x,t)-\rho_0 = \frac{1}{4\pi a_\infty^2}\frac{\partial^2}{\partial x_i \partial x_j}\int_V \frac{T_{ij}}{r}dV(y) - \frac{1}{4\pi a_\infty^2}\frac{\partial}{\partial x_i}\int_S \frac{n_j}{r}\left(p\delta_{ij}-\tau_{ij}\right)dS(y) \tag{3.6}$$

The first part of the right side of the equation is the volume contribution and the second part is the surface contribution. In this equation x is the observer position and y is the source position and r is the distance between them.

It is important to state that both Curle and Lighthill made no simplifying assumptions in their analogies that are exact. Curle (1955) states in his work that the presence of the solid boundaries can be observed in two ways:

1. The sound generated by the quadrupoles will be reflected and diffracted by the solid boundaries.

2. There might be a resultant distribution of dipoles at the boundaries.

To apply the turbulent flows to Curle's Analogy which is exact with no simplifying assumptions, three important assumptions are made.

First is to state the independence of the source term T_{ij} on acoustic field. Second is assuming the isotropic wave operator describes the propagation of sound accurately. And third is locating the observer in a region where flow is isentropic.

The accuracy of the first assumption is not valid mathematically, as the density term appears on the both sides of the equation. However physically, hydrodynamic phenomenon produces the sound which are almost independent of acoustic phenomenon.

When the flow is stagnant the second assumption becomes valid. This assumption becomes really good in low Mach number flows as in our case, since the convection effects are a factor Mach slower than the propagation of the acoustic wave.

If the observer is in the isentropic flow region, the density fluctuation at the observer position can be given as:

$$\rho(x,t) - \rho_0 = \frac{p(x,t) - p}{a_\infty^2} \tag{3.7}$$

As the temporal form of Curle's solution is less sensitive to numerical errors, to transform spatial derivatives to temporal ones is more advantageous. Larsson et al. (2004) transformed the spatial derivative in to temporal one by applying chain rule:

$$\frac{\partial f(\tau)}{\partial x_i} = \frac{\partial f}{\partial \tau}\frac{\partial \tau}{\partial x_i} = -\frac{1}{a_\infty}\frac{\partial r}{\partial x_i}\frac{\partial f}{\partial \tau} \tag{3.8}$$

In the same work the equation below is used for the unit vector directed from the source point y to listener x.

$$\frac{\partial r}{\partial x_i} = \frac{\partial \sqrt{(x_j - y_j)^2}}{\partial x_i} = \frac{(x_i - y_i)}{\sqrt{(x_j - y_j)^2}} = \frac{x_i - y_i}{r} = l_i \tag{3.9}$$

The usage of the later equation yields:

$$\begin{aligned} p(x,t) - p_0 =& \frac{1}{4\pi}\frac{\partial}{\partial x_i}\int_V -l_i\left[\frac{\dot{T}_{ij}}{a_\infty r} + \frac{T_{ij}}{r^2}\right] dV(y) \\ & - \frac{1}{4\pi}\int_S -l_i n_j\left[\frac{\dot{p}\delta_{ij} - \dot{\tau}_{ij}}{a_\infty r} + \frac{p\delta_{ij} - \tau_{ij}}{r^2}\right] dS(y) \\ =& \frac{1}{4\pi}\int_V \left(l_i l_j\left[\frac{\ddot{T}_{ij}}{a_\infty^2 r} + 2\frac{\dot{T}_{ij}}{a_\infty r^2} + 2\frac{T_{ij}}{r^3}\right] - \frac{\partial l_i}{\partial x_i}\left[\frac{\dot{T}_{ij}}{a_\infty r} + \frac{T_{ij}}{r^2}\right]\right) dV(y) \end{aligned} \tag{3.10}$$

By including the derivative of the unit vector which is given below the equation after is obtained.

$$\frac{\partial l_j}{\partial x_i} = \frac{\partial}{\partial x_i}\left[\frac{x_j - y_j}{r}\right] = \frac{\delta_{ij} - l_i l_j}{r} \tag{3.11}$$

$$\begin{aligned} p(x,t) - p_0 =& \frac{1}{4\pi}\int_V \left[\frac{l_i l_j}{a_\infty^2 r}\ddot{T}_{ij} + \frac{3l_i l_j - \delta_{ij}}{a_\infty r^2}\dot{T}_{ij} + \frac{3l_i l_j - \delta_{ij}}{r^3}T_{ij}\right] dV(y) \\ & + \frac{1}{4\pi}\int_S \left[l_i n_j \frac{\dot{p}\delta_{ij} - \dot{\tau}_{ij}}{a_\infty r} + \frac{p\delta_{ij} - \tau_{ij}}{r^2}\right] dS(y) \end{aligned} \tag{3.12}$$

Although the viscous tangential stresses and entropy variations are important near the walls, generally these phenomena are overwhelmed by the normal stresses and neglected. Also the flow can be assumed isothermal (or isentropic) and compressibility effects are negligible in the flow. So the differences between the exact pressure field $p\delta_{ij}$ and the approximate one $a_\infty^2 \rho_{ij}$ become unimportant. These assumptions yield to a mathematical presentation of the Lighthill stress tensor:

$$T_{ij} = \rho v_i v_j \tag{3.13}$$

This can be explained as the principal generators of sound are the fluctuating Reyndols stresses. So the solution to Curle's Analogy now becomes:

$$p(x,t)-p_0 = \frac{1}{4\pi}\int_V \left[\frac{l_i l_j}{a_\infty^2 r}\ddot{T}_{ij} + \frac{3l_i l_j-\delta_{ij}}{a_\infty r^2}\dot{T}_{ij} + \frac{3l_i l_j-\delta_{ij}}{r^3}T_{ij}\right] dV(y) + \frac{1}{4\pi}\int_S \left[l_i n_j \frac{\dot{p}\delta_{ij}}{a_\infty r} + \frac{p\delta_{ij}}{r^2}\right] dS(y) \tag{3.14}$$

Parkhi (2009) showed with an efficiency of sources analysis that the volumetric sources can be negligible with a near field sound prediction, and Haigermoser (2009) suggested that when the data gathered are only available in 2D plane, Modified Curle'd Analogy can be integrated from $-w$ to w and which yields a 1D integral equation:

$$p(x,t)-p_0 = \frac{1}{4\pi}\int_S l_i n_j \left[2arctan\left(\frac{w}{r}\right)\frac{\dot{p}\delta_{ij}}{a_\infty} + 2w\frac{p\delta_{ij}}{r^2}\right] dL(y) \tag{3.15}$$

Applying the simple trapezoidal rule this integral yields to:

$$SP(x,k) = \frac{1}{4\pi}\sum_i^n \left[L(i)N(i)\left(2arctan^{-1}\left(\frac{w}{R(i)}\right)\frac{\dot{(p)}(i,k)}{c_0} + 2w\frac{p(i,k)}{R(i)^2}\right)\right]\Delta S(i) \tag{3.16}$$

In this equation pressures gathered from the walls of the cavity used to obtain sound pressure at desired listener locations. Sound pressure levels are calculated with the equation below:

$$SPL = 10log_10\left(\frac{p_{rms}^2}{p_{rms}^2}\right) \tag{3.17}$$

where $p_ref = 20\mu Pa$.

4. CFD INVESTIGATION

4.1 Introduction

The first step of calculating the noise levels radiated from a cavity flow is to gather the pressure fluctuations from the cavity walls. After that the unsteady pressure data obtained from the cavity walls, will be used in the equation acquired in the previous chapter. To obtain the pressure data CFD analysis is going to be conducted. This data can also be obtained by experimental investigations, but as the author‘s ambition is to improve this work and solve the problem with a homemade source code, it seemed more wise to solve the problem in a commercial CFD tool.

The investigations will include four different geometries. The analyses are solved with a solver using Reynolds Averaged Navier Stokes method, Implicit Unsteady Solver, Segregated Flow and Realizable Two Layer $k-\varepsilon$ Turbulence approach. Detailed explanations of these approaches and methods, and other options could be used is given in following sections. It is important to remind here that this work is investigating the geometrical effects in cavity flow noise generations. The boundary conditions and physical conditions of the flow will be same for all the analyses conducted.

4.2 Cavity Geometries

There are four different geometries that are analyzed through the work. First geometry is a simple cavity with the $\frac{L}{D}$ ratio of 2. Geometrical properties of the cavities can be seen in Figure 4.1, Figure 4.2, Figure 4.3 and Figure 4.4. L of the cavity is 0.30 m and D is 0.15 m.

The radii given to the leading and trailing edges have the same dimensions to investigate the place of the radii better.

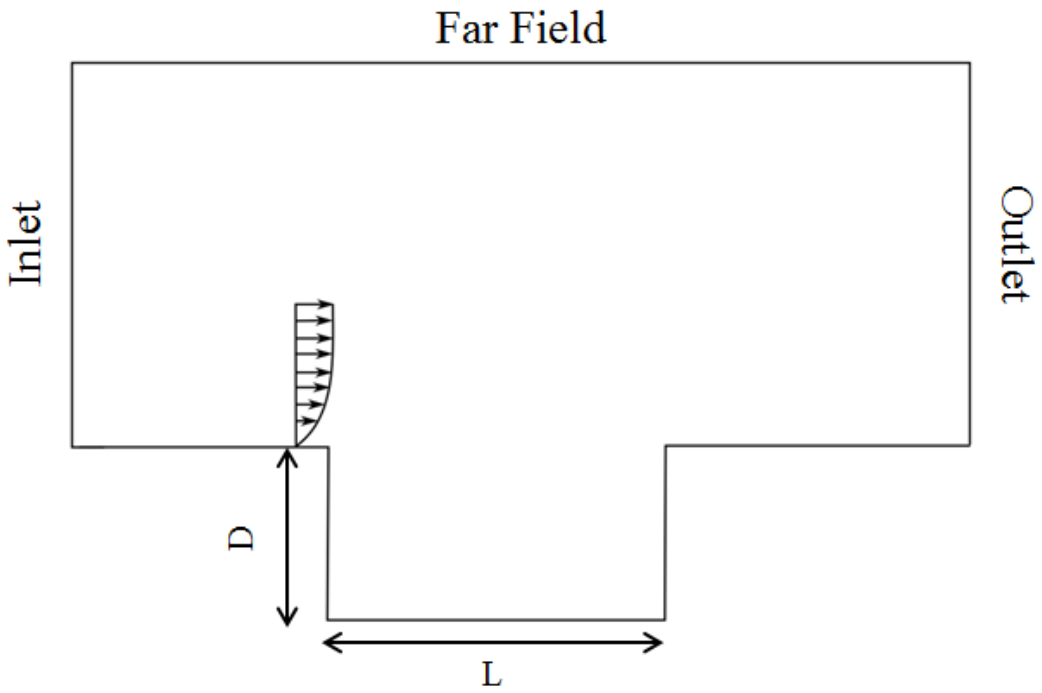

Figure 4.1: Case 1 – Validation case with no rounded edges.

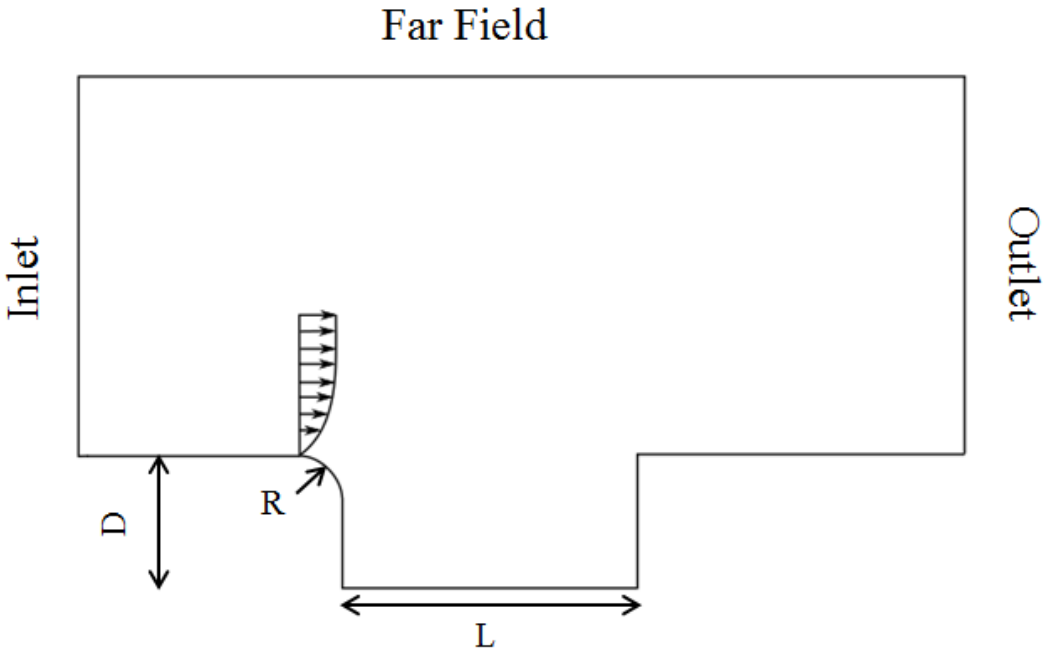

Figure 4.2: Case 2 – Rounded leading edge.

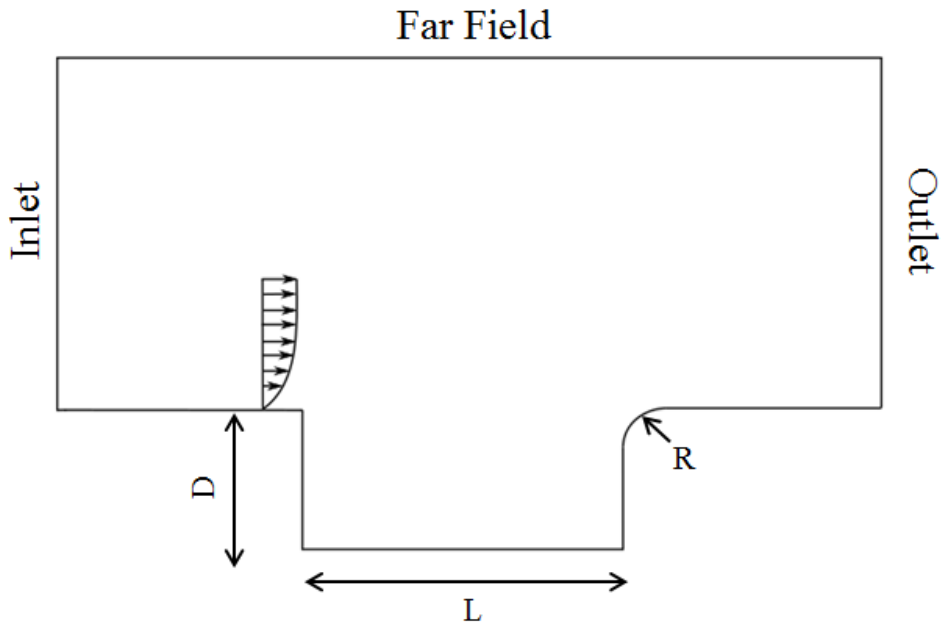

Figure 4.3: Case 3 – Rounded trailing edge.

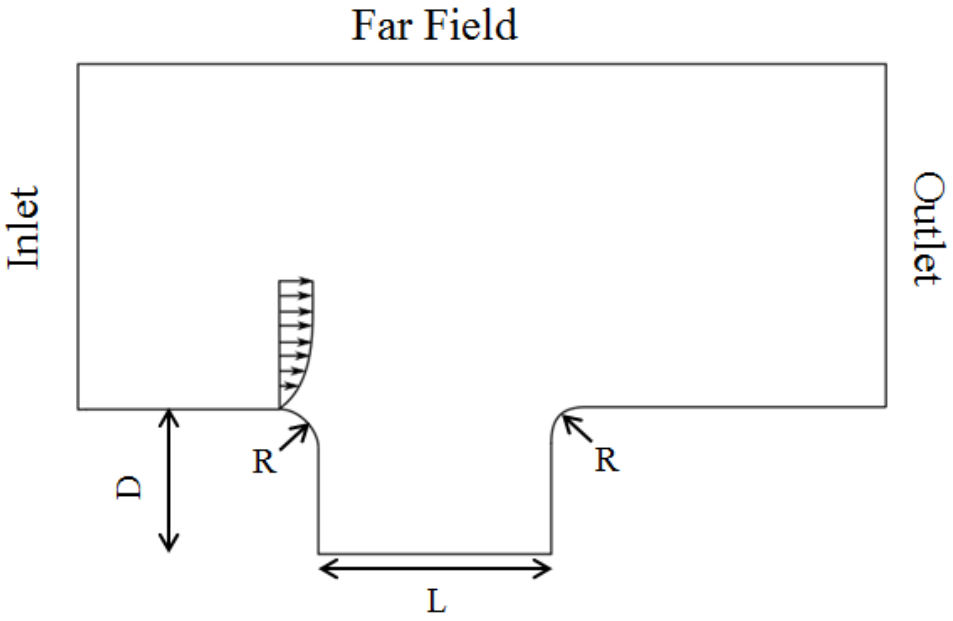

Figure 4.4: Case 4 – Rounded leading and trailing edge.

4.3 Mesh Properties

Mesh quality is highly important to get an efficient and accurate solution to the problem. The quality of the mesh is dependent basically on the rate of convergence, solution accuracy and CPU time required. The rate of convergence shows the speed of the mesh to achieve the correct solution. To obtain a good rate of convergence the mesh should apprehend the important phenomena of the flow like boundary layers or shock waves. In the case of cavity flow, boundary layer is highly important in both 5 walls

of the geometry. The boundary layer in the upstream and downstream wall affects the solveability of the shear layer separation and impingement drastically. This issue for an example led this work to several steps of iterations in mesh generation. Solution accuracy is maybe the most important feature that determines the quality of the mesh, as gathering wrong solutions have zero use except misleading the investigation. To get good solution accuracy, certain areas in the geometry should be finer where the gradients of the field solved are higher. In the case of the cavity flow, mesh around the edges and in the cavity should be finer as the velocity and pressure gradients are significantly higher than other parts of the flow area. Other important is CPU time required which should be decreased as much as possible. It is useful to adjust the mesh density to provide the previous features and have the least CPU time possible. It is rational to have unnecessary mesh elements that do not have any improving effect on neither the solution accuracy nor the rate of convergence. Meshes used in all of the cases have structured grids which have the cell shape of hexahedron. Mesh used in the validation case can be seen in Figure 4.5.

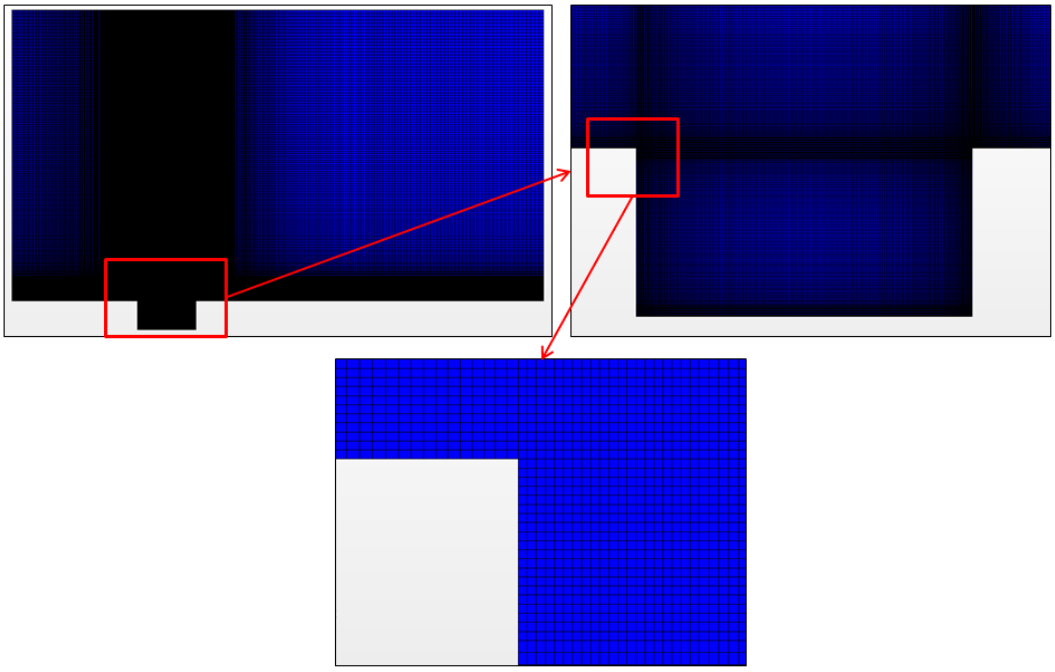

Figure 4.5: Mesh of the validation case.

4.4 Modelling Physics

In this section, CFD model used in this thesis is described including detailed explanations of flow and energy, turbulence and boundary conditions. It is useful to say that the flow is 3-dimensional, unsteady, and adiabatic and the domain has no motion like translation or rotation. As an addition, initial conditions are given as the domain is ambient. These physical properties are clear and need no further explanation.

4.4.1 Modelling flow and energy

In all of the fluid dynamics problems, the physics model is based on principles which are; mass is conserved, Newton's second law and energy is conserved. The form of the fundamental governing equations of fluid dynamics, the continuity, momentum and energy equations which are called the conservation equations, used in CFD is Navier-Stokes equations.

With the finite volume method these equations transform in to equations that can be solved numerically. To solve this equations two approaches, segregated approach and coupled approach are used. In segregated approach flow equations are solved one after the other and are only linked with a correction equation. In coupled approach the system of equations are coupled and solved simultaneously. Choosing one of these approaches is important for the problem to be solved accurately, easily and effectively. They have many different relative strengths and weaknesses regarding what the problem is. The coupled algorithm requires more memory then segregated algorithm as it solves all the equations in one time. In compressible flows, particularly problems including shocks, coupled algorithm provides more robust and accurate solutions. But in incompressible flows it is wiser to select a segregated flow as it needs lower computational resources. In this work segregated flow model is selected to solve the Navier-Stokes equations. This model is more efficient in incompressible flows with the usage of constant density. With segregated flow approach implicit unsteady method is used for modelling time and the time-step used is 10^{-7}. In unsteady flows explicit solvers use only data from the previous step to solve the current step, while implicit solvers use data from both previous and current step.

4.4.2 Modelling turbulence

4.4.2.1 Introduction

When the fluid systems reach a value above the so called critical number Re_crit, The flow starts to flow characteristics start to change radically. This leads to a flow behaviour of randomness and chaos. All of the flow properties like velocity and pressure changes in both time and place chaotically and randomly even with constant boundary conditions. Flow regime with these properties is referred as turbulent flow, with an example which can be seen in Figure 4.6 (Versteeg and Malalasekra, 2007).

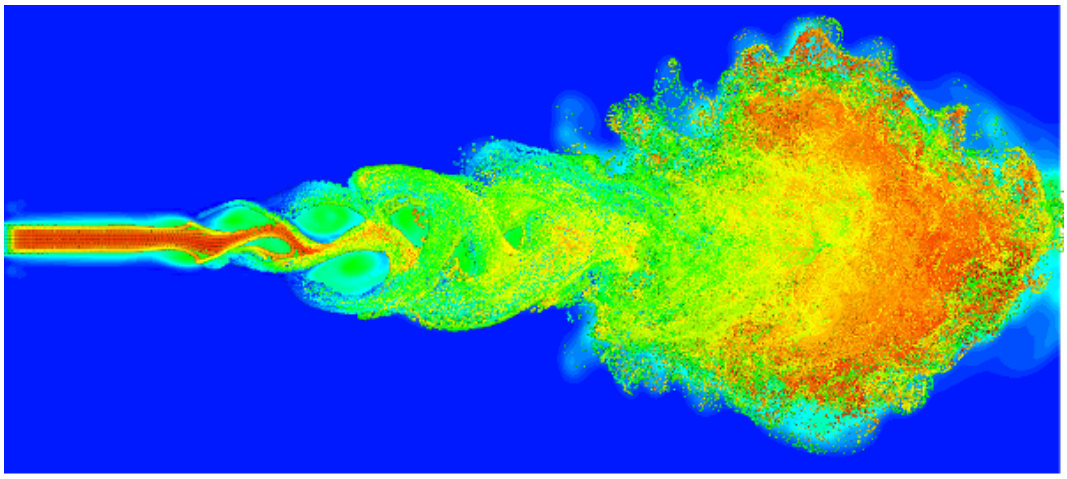

Figure 4.6: Turbulent flow.

The nature of turbulent is very random and within it many different length scales are included. The velocity has fluctuations within different scales. In Reynolds decomposition, these fluctuations are depicted with an additional component added to the mean velocity. This allows characterizing the turbulent flow with mean values and statistical properties of their fluctuations both in velocity, pressure and other unsteady flow properties. These fluctuations in turbulent flows have three-dimensional spatial character, which is another complexity of this regime. As summary turbulent flows are chaotic, random, 3-dimensional, time dependent, have mixing characteristics and most importantly it is a property of the flow, not the fluid. As stated in the previous paragraph turbulent flows have vortices in many different sizes from large ones to small ones. Main scales of these vortices are the large scale, the integral scale, the Taylor micro-scale and the Kolmogorov(dissipation) scale. Large scales like integral scale is defined by the geometry of the flow like pipe diameter, size of

the wind-tunnel and boundary layer thickness. Small scales though, are defined by viscosity. At very small length scales, viscosity tend to smooth out local velocity gradients. Thereby, preventing generation of infinitely small scales. Turbulence kinetic is lost or "dissipated" at a rate of "ε" per unit mass into heat with time. Interaction between large scales and small scales are non-linear in nature. With a good approximation, it can be told that mainly energy is transmitted from large scales to small scales. The vorticity of small scale eddies are much larger than that of the larger scale motions. On the other hand, the small scale energy is significantly small compared to larger scale energy.

4.4.2.2 Turbulence models

Modelling the turbulence is an interesting but a difficult objective to reach. Many researches paid immense attention on it and it is seen that there are no recent hope for a simple analytical theory to calculate the interested properties of the flow. So the investigations directed to use the power of digital computers to obtain the fundamental results. It is discussed in the previous section that there are many difficulties about modelling arise within the turbulent region. Most important of them is the pressure-gradient term in the Navier-Stokes equations, which is non-linear and non-local when it is expressed in terms of velocity (Pope, 2000). There are different simulation approaches for modelling turbulent flows, main of them being Reynolds-Averaged Navier-Stokes (RANS), large-eddy simulation (LES) and direct numerical solution (DNS). DNS solves the Navier-Stokes equation including all the scales of the flow, using appropriate initial and boundary condition. It became a feasible approach after computers with enough power designed. But it is not an efficient approach yet, so it is better to think twice before using DNS. It is a very basic and accurate approach, providing detailed knowledge about the flow, like the Lagrangian statistics and statistics of pressure fluctuations which are not possible to obtain experimentally, but the cost of using is significantly high and the computers are not powerful enough to solve high Reynolds number flows. Reynold-averaged Navier-Stokes (RANS) models solve the Reynolds equations for the mean velocity field. The Navier-Stokes equations are time or ensemble averaged resulting extra terms that modelled with classical turbulent models like $k-\varepsilon$, $k-\omega$ and Spalart-Allmaras model. In engineering, this model is mostly use because of its modest computing

resource requirement and accurate results. In commercial CFD codes RANS is pretty common and basically there are different turbulence calculation procedures with different extra transport equations included. Mixing length model does not use extra transport equations. Spalart-Allmaras model uses one extra transport equation, while $k-\varepsilon$ and $k-\omega$ uses two extra transport equations. Mixing length models try to use simple formulae for dynamic viscosity term as a function of position to explain the stress terms. $k-\varepsilon$ model is an approach of describing the turbulent flow in the means of transport of turbulence using convection an diffusion, and also the production and destruction turbulence. For doing it a transport equation for the turbulent kinetic energy k and another transport equation for the rate of dissipation of turbulent kinetic energy ε is solved, which makes the model more accurate but costly. In $k-\omega$ model ω the turbulence frequency is used as the second variable which is proposed by Wilcox (1988). The positive feature of this model is that it does not need wall damping functions in low Reynolds number applications. But it is seen by Menter(1992) that the model is dependent on the free stream value of ω, which is a serious problem. So he propose SST $k-\omega$ model which includes improvements like revised model constant, blending functions and limiters (Versteeg and Malalasekra, 2007). Large eddy simulation handles the large and smaller eddies with different approaches, computing large eddies with a time-dependent simulation and capturing smaller eddies with a compact model. This is because the behavior of the large and small eddies having significant differences. The larger eddies, can be counted as anisotropic having interaction with the mean flow and they are dependent on both the geometry of the domain, the boundary conditions and body forces. To separate the larger and smaller eddies; spatial filtering operation is used in LES. LES has a better ability to describe unsteady flows and large-scale turbulent structures. However, LES becomes more costly in wall-bounded flows. It is suggested to use LES near-wall modelling if it is necessary to use LES (Pope, 2000). For a final remark, it is useful to state that both of these applications can be used in many different applications with many different outcomes, eases and problems. Turbulent-flow problems are hard, challenging but worthwhile for research efforts and it is important to determine the problem and required outcomes before deciding a solution approach. In this thesis Reynolds-Averaged Navier-Stokes(RANS), two-layer all $y+$ wall treatment and realizable $k-\varepsilon$ model is used. $k-\varepsilon$ model is selected because it has both fair

properties of robustness, computational cost and accuracy and this model has good solutions for complex recirculation problems. Realizable $k-\varepsilon$ model is developed by Shih et al. (1994), which lets the model satisfy certain mathematical constraints on the normal stresses consistent with experimental observations in boundary layers buy using a critical coefficient which is expressed as a function of mean flow and turbulence properties. All $y+$ wall treatment is a near-wall modeling assumption for each turbulence models that uses a hybrid treatment that includes both the assumption of near-wall cells lying within the logarithmic region of the boundary layer and the assumption of the viscous sub-layer being resolved properly. Two-layer approach is an approach which is suggested by Rodi (1991), which divides the computation in two layers. The turbulent dissipation rate and the turbulent viscosity are specified as the functions of wall distance in the layer next to the wall.

4.5 Boundary Conditions

The boundary types of the cavity can be seen in Figure 4.7. The inlet velocity magnitude is 12 m/s and the outlet pressure is 1 atm.

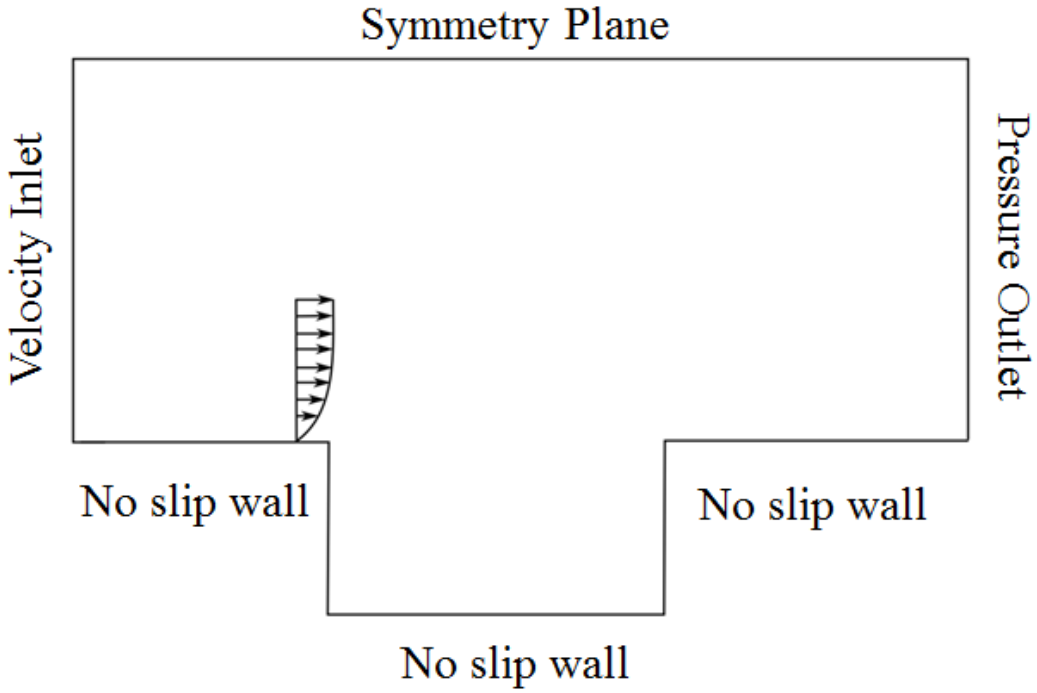

Figure 4.7: Boundary types.

The velocity at the inlet is 12 m/s and the pressure at the outlet is 1 atm. At the farfield side of the domain symmetry plane boundary condition is given. It means, on that boundary domain is extended as a mirror of the actual domain. As the flow is steady at

farfield this approach is convenient for this case. Symmetry plane is given to the third dimension walls of the domain.

5. RESULTS AND DISCUSSION

Validation is done with the thesis of Parkhi (2009) "Aeroacoustics of Cavity Flow Using Time Resolved PIV". He tried to predict the sound produced over a rectangular cavity by measuring two dimensional flow fields using a technique called Temporally-Resolved Particle Image Velocimetry. He measured the velocity data of the two dimensional of the flow then fed it into a planar pressure solver to obtain pressure fields. At the end, he compared the results gathered from the analogies and microphone measurements. The results are given in two parts, CFD and aeroacoustic. In CFD results, unsteady velocity fields and pressures obtained from several locations at the end of the analyses are given. In aeroacoustic results, sound pressure, OASPL data and power spectrum of the SPL data are given at several listener locations.

5.1 CFD Results

5.1.1 Validation results

Streamlines and normalized velocity fields have good correlation with the validation cases. The nature is very close but values are a bit higher. This because the case of Parkhi (2009) which these datas are obtained has the free stream velocity of 10 m/s. So it is logical to have higher values then the results of the validation case. In normalized velocity vector plots, streamwise and vertical velocities are normalized with the freestream velocity of 12 m/s. Velocity streamline comparison can be seen in Figure 5.1. Figure 5.2 shows the normalized streamwise velocity field comparison and Figure 5.3 shows the normalized vertical velocity field comparison.

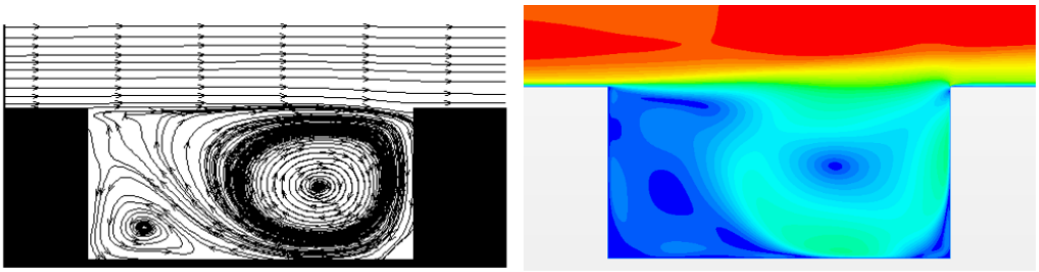

Figure 5.1: Velocity vectors with line integral convolution; Left: Streamlines from Parkhi(2009), Right: Case 1.

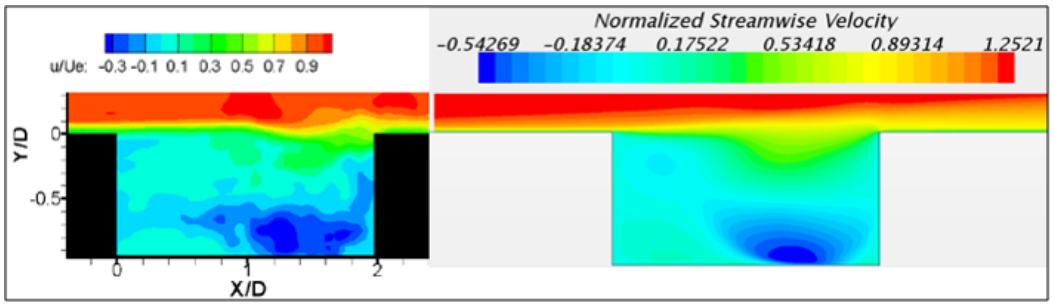

Figure 5.2: Normalized streamwise velocity fields; Left: Parkhi(2009), Right: Case 1.

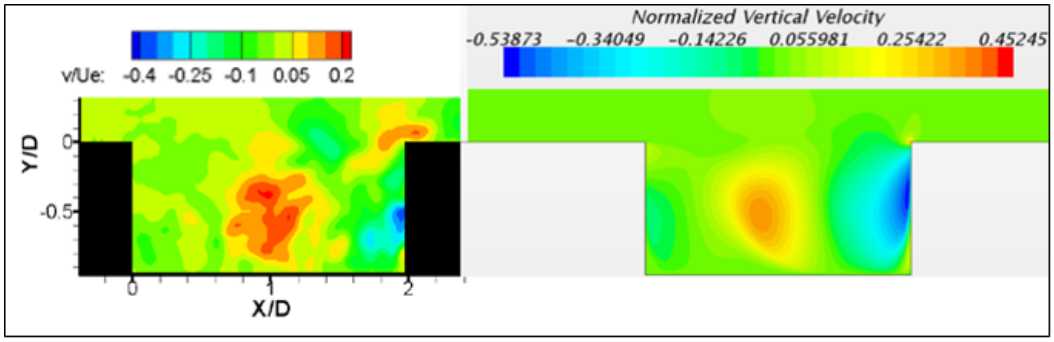

Figure 5.3: Normalized vertical velocity fields; Left: Parkhi(2009), Right: Case 1.

5.1.2 Unsteady flow field

In this section velocity magnitude fields are given figures below. Figure 5.4 shows the comparison between the validation case and the case with rounded leading edge case. Figure 5.5 is the comparison between validation and rounded trailing edge cases. The comparison between the validation case and the case with both edges rounded is shown in Figure 5.6.

Figures shows us that rounding the leading edge delays the vortex generation and the flow attaches to the surface of the upstream wall for a longer time compared to the validation case. In rounded trailing edge rounded case it can be seen that the vortex hitting to the trailing wall is softened noticeably and a bigger area with lower velocities occur. Case with both edges shows the features of both former cases.

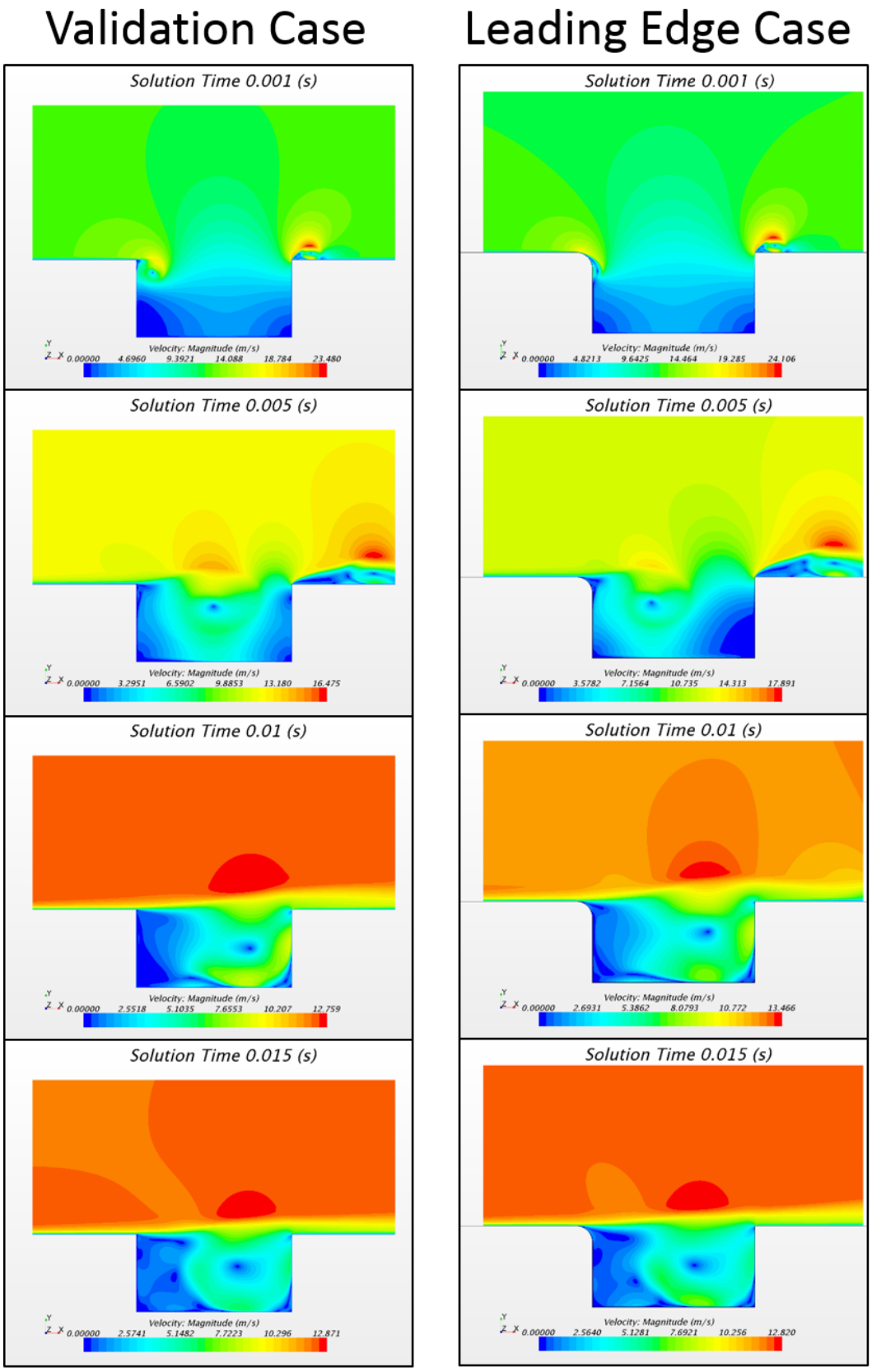

Figure 5.4: Comparison of velocity magnitudes of validation and leading edge cases.

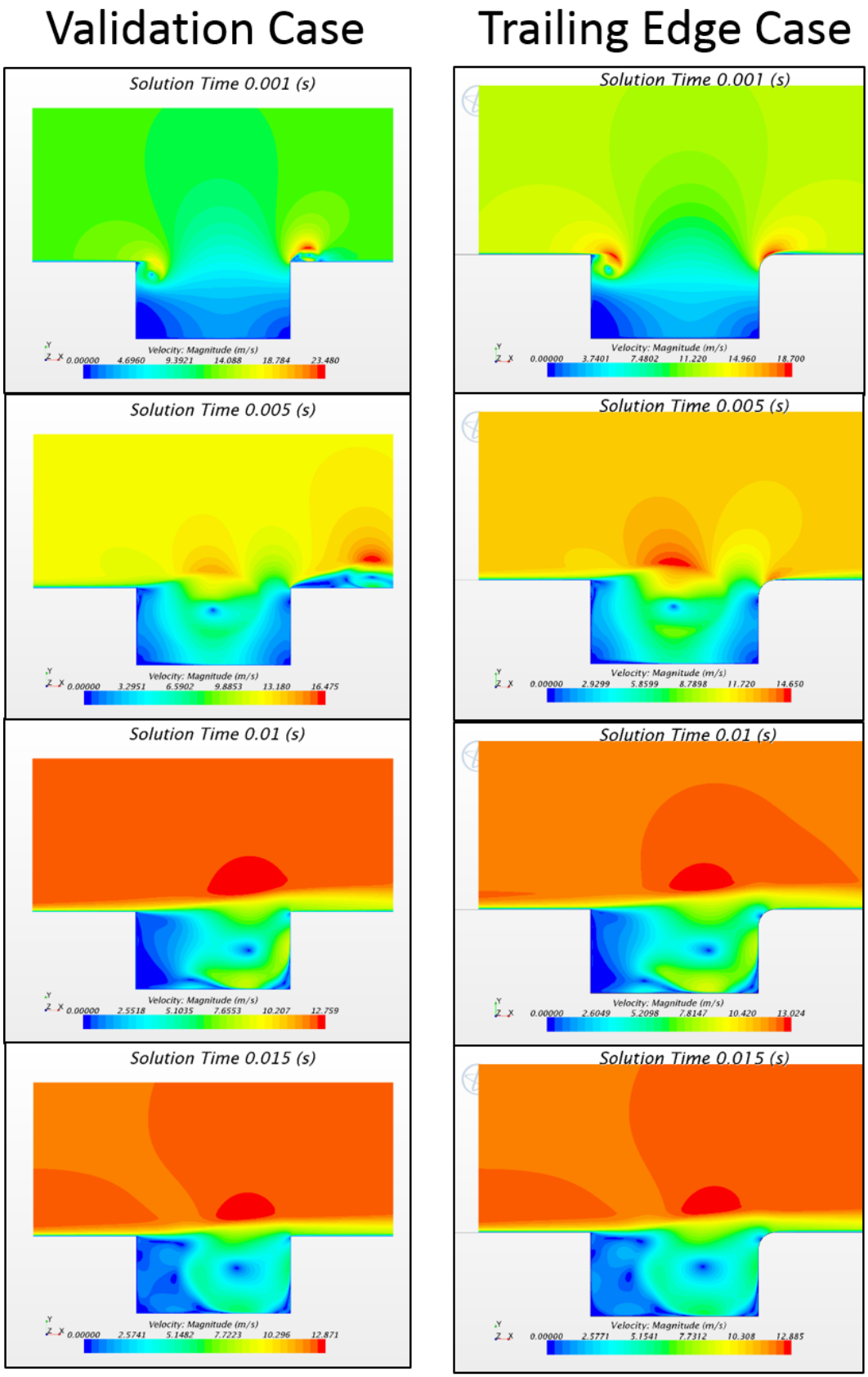

Figure 5.5: Comparison of velocity magnitudes of validation and trailing edge cases.

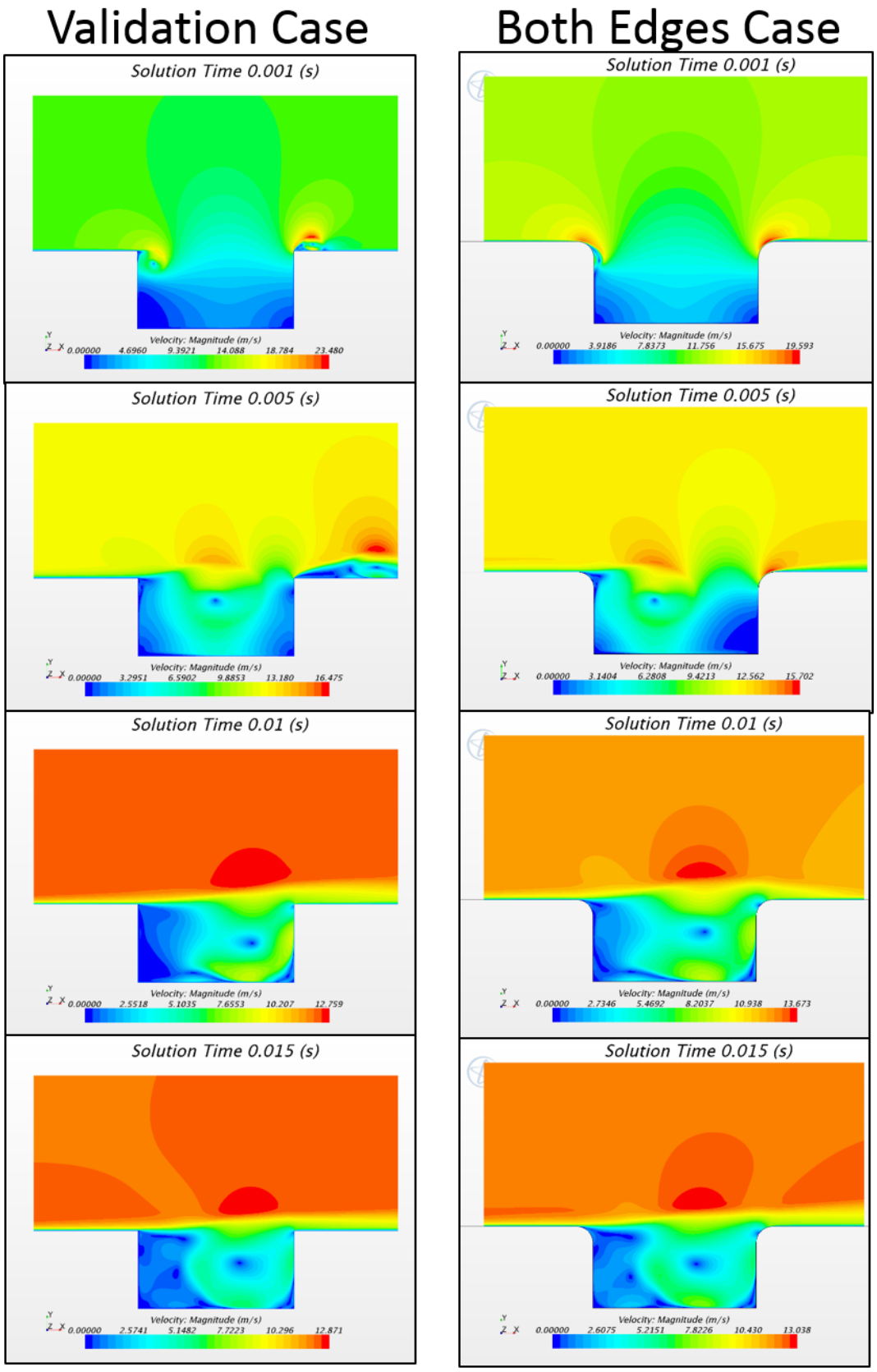

Figure 5.6: Comparison of velocity magnitudes of validation and both edges cases.

5.1.3 Normalized pressure field

In this section normalized pressure fields are given in all cases at different solution times. Fields at 0.0005 seconds, 0.001 seconds, 0.05 seconds, 0.01 seconds and 0.015 seconds can be respectively seen in Figure 5.7, Figure 5.8, Figure 5.9, Figure 5.10 and Figure 5.11. Normalized pressure fields show the same features with the velocity magnitude fields naturally. As stated before with the leading edge rounding the vortex propagation delays and higher pressure values are observed at the upstream wall for a longer time. In trailing edge case lower pressure distributions at the trailing edge surface can be observed. For the both edge rounded case vortex delay is observed same with the leading edge case and pressure distributions have both features of the former two cases. These pressure distributions effects the sound generation significantly as the sound at the listeners are calculated using the pressure data obtained from the surface at every time step.

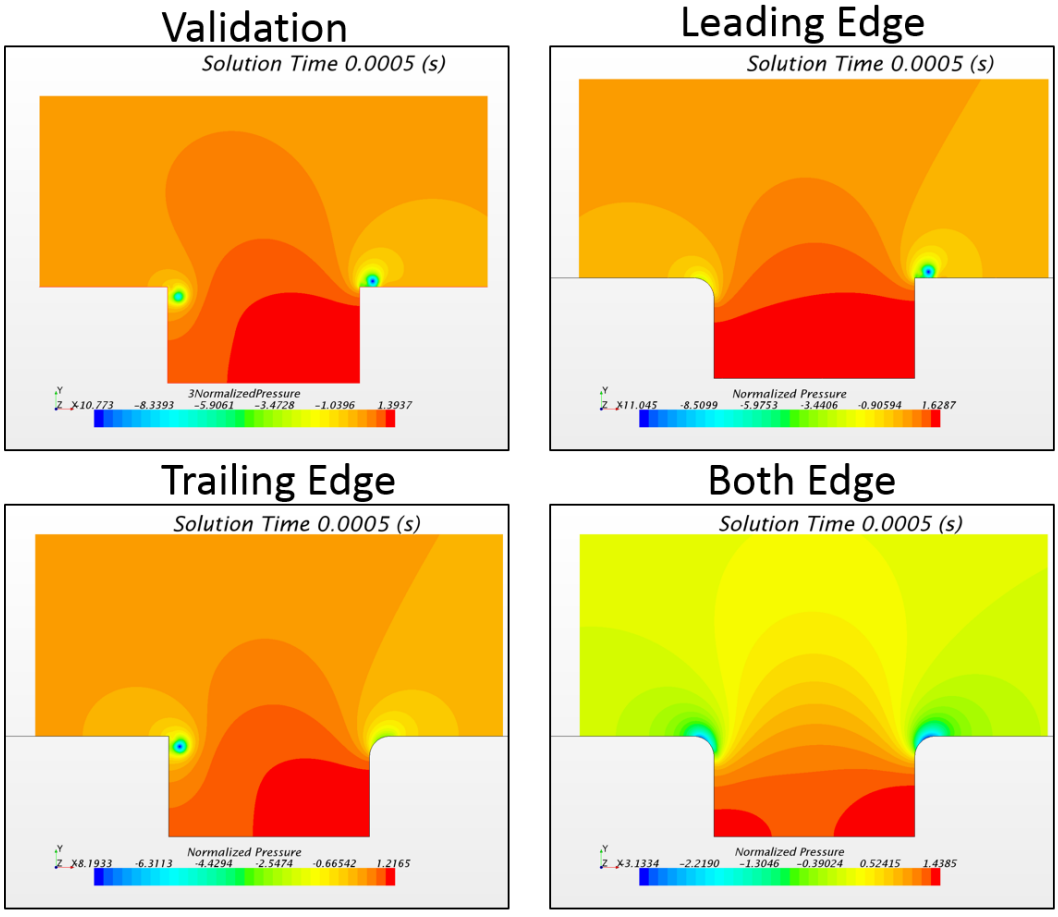

Figure 5.7: Comparison of normalized pressure distributions of all cases at physical time of 0.0005 s.

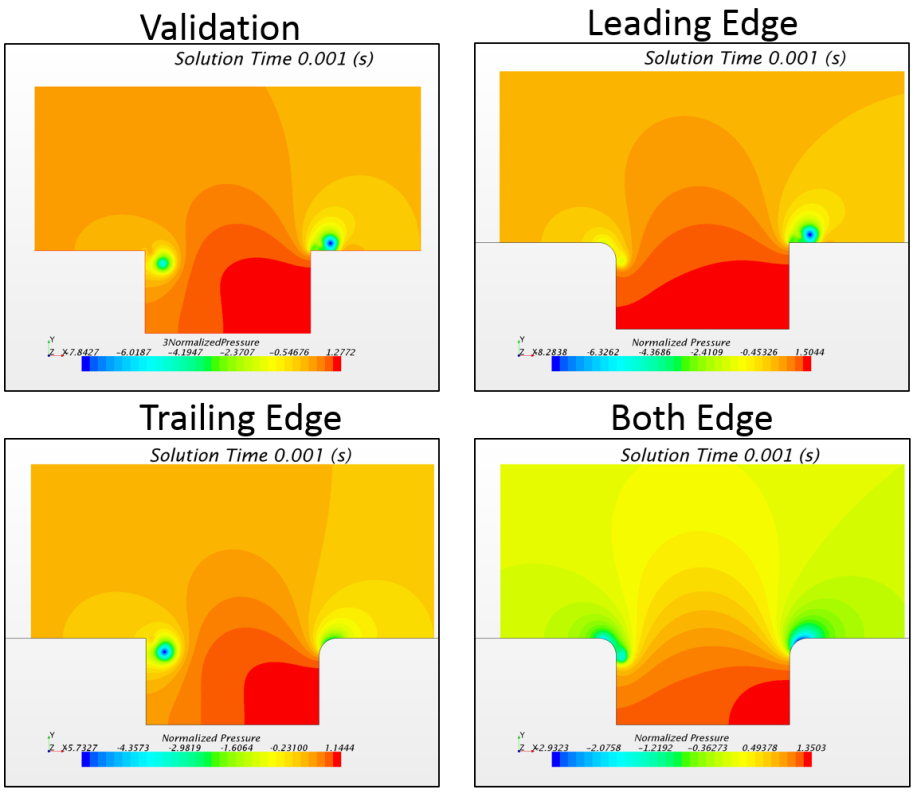

Figure 5.8: Comparison of normalized pressure distributions of all cases at physical time of 0.001 s.

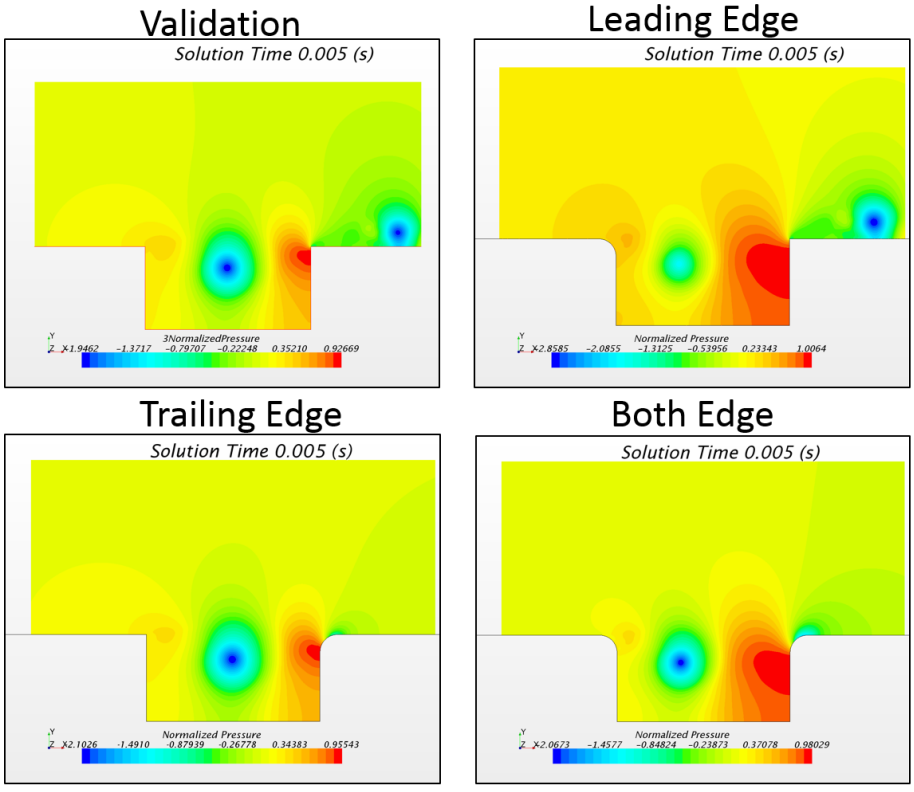

Figure 5.9: Comparison of normalized pressure distributions of all cases at physical time of 0.005 s.

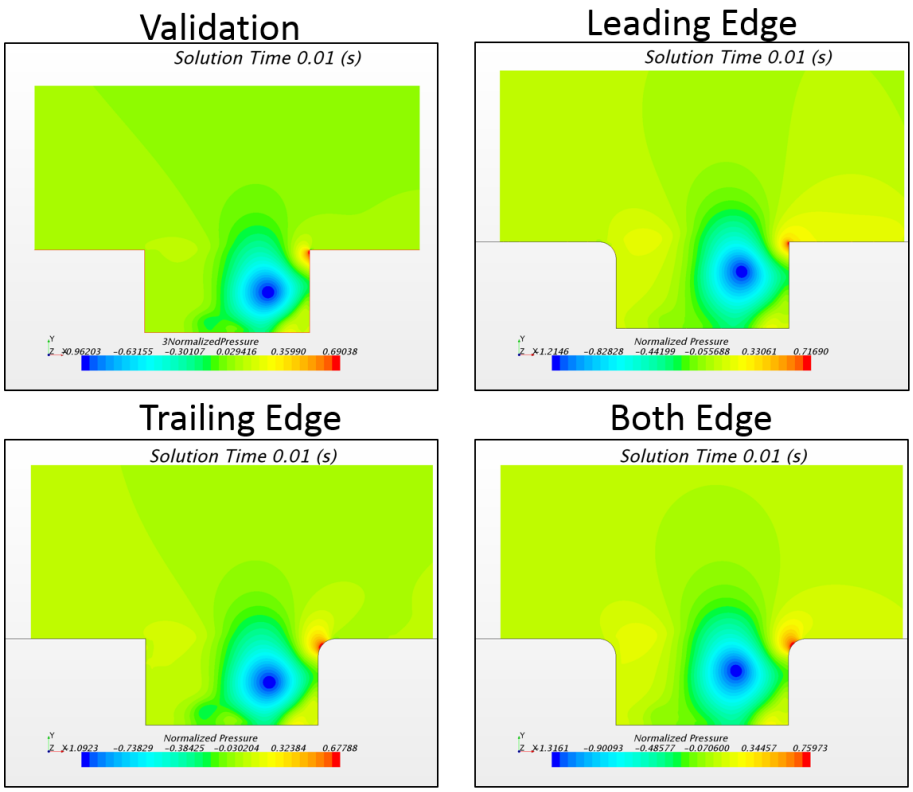

Figure 5.10: Comparison of normalized pressure distributions of all cases at physical time of 0.01 s.

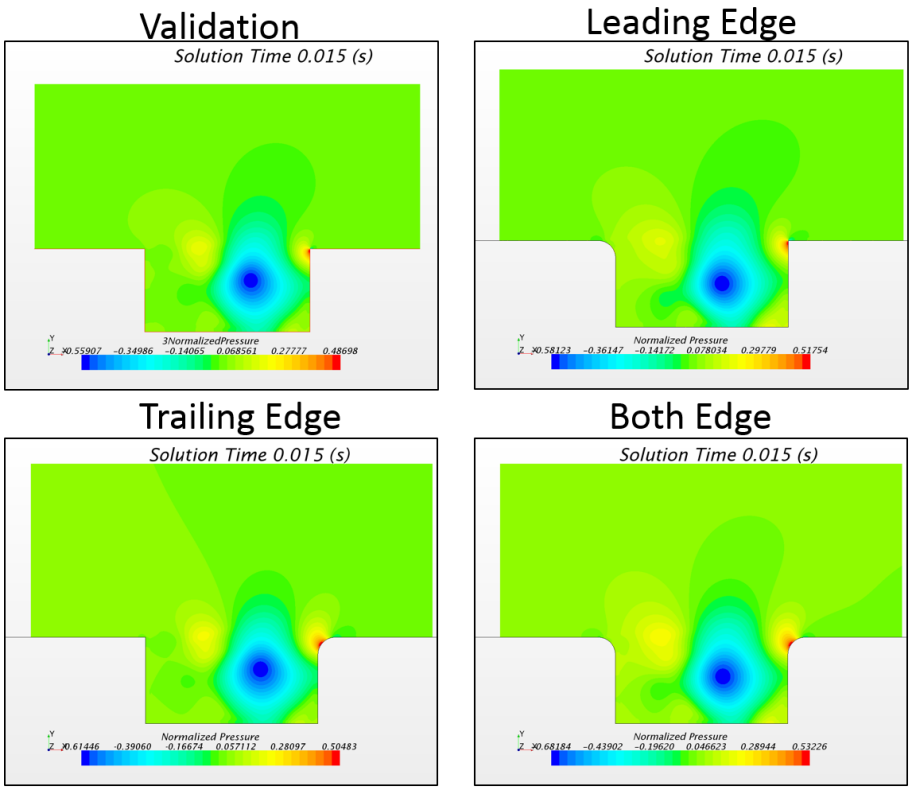

Figure 5.11: Comparison of normalized pressure distributions of all cases at physical time of 0.015 s.

5.1.4 Aeroacoustic Results

In the aeroacoustic results sound pressures calculated at the listener locations, which can be seen in Figure 5.12, with home-made code using the Equation 3.16. Sound pressures at listeners 1,2 and 3 can be seen at Figure 5.13 and sound pressures at listener 4,5 and 6 can be seen in Figure 5.14. From these figures it can be seen that sound pressure at all listeners have the same damping nature, which is natural as the pressure data used in the code is same for all the listeners. The only difference is the values. Further listeners have lower values as R at Equation 3.16 gets bigger. It is important to state that the angle between the source and the listener is important too. As the angle gets away from 90 degrees, sound pressures drop.

Power spectrum of sound pressure levels are given in Figure 5.15 and Figure 5.16. It can be seen that for all listeners maximum sound pressure levels are seen at leading edge rounded case. It can be explained with the flow features given in the previous section. As the higher pressure values follows the cavity flow more, it gives higher sound pressure levels. The least sound pressure levels can be seen at trailing edge rounded case. It can be explained with the flow features, as the vortex hit on the trailing wall is softened by the rounding and lower pressure values are observed at cavity trailing wall. Both edges rounded case is between these two cases, closer to leading edge rounded case.

At last, overall averaged sound pressure levels are given at Figure 5.17. It can be seen that listeners which are closer to the source and have angles closer to 90 degrees with the source have higher OASPL values. In addition, at listeners 4, 5 and 6 experimental results obtained by Parkhi (2000) can be seen. The values are close enough to the experimental results, as the home-made code uses an equation with lots of modifications. Finally, it can be seen leading edge rounded case have the highest OASPL values at all listeners followed by both edges rounded case and validation case. Trailing edge rounded case have the lowest OASPL values.

Additionally, it should be stated that in power spectrum of sound pressure levels, more dense graphics with several peaks were expected. The given sound pressure level graphics show damping natures which are expected but the linearity of this damping

was not expected. This might be because of the turbulence model used at the CFD analysis. The peaks in these power spectrum graphics would show the dominant frequencies. These frequencies are investigated by Rossiter (1964) by conducting several wind-tunnel experiments. He tried to predict the dominant frequencies by using a semi-empirical formula given below:

$$St = \frac{fL}{U} = \frac{n-a}{\frac{1}{\kappa}+M} \tag{5.1}$$

In this formula, f is the frequency tones, U is the free-stream velocity, L is the length of the cavity, n is the mode number, M is the Mach number, κ is the ratio of convection velocity of vortices to free-stream velocity and a is the spacing between vortices. With future investigations dominant frequencies should be checked with this formula.

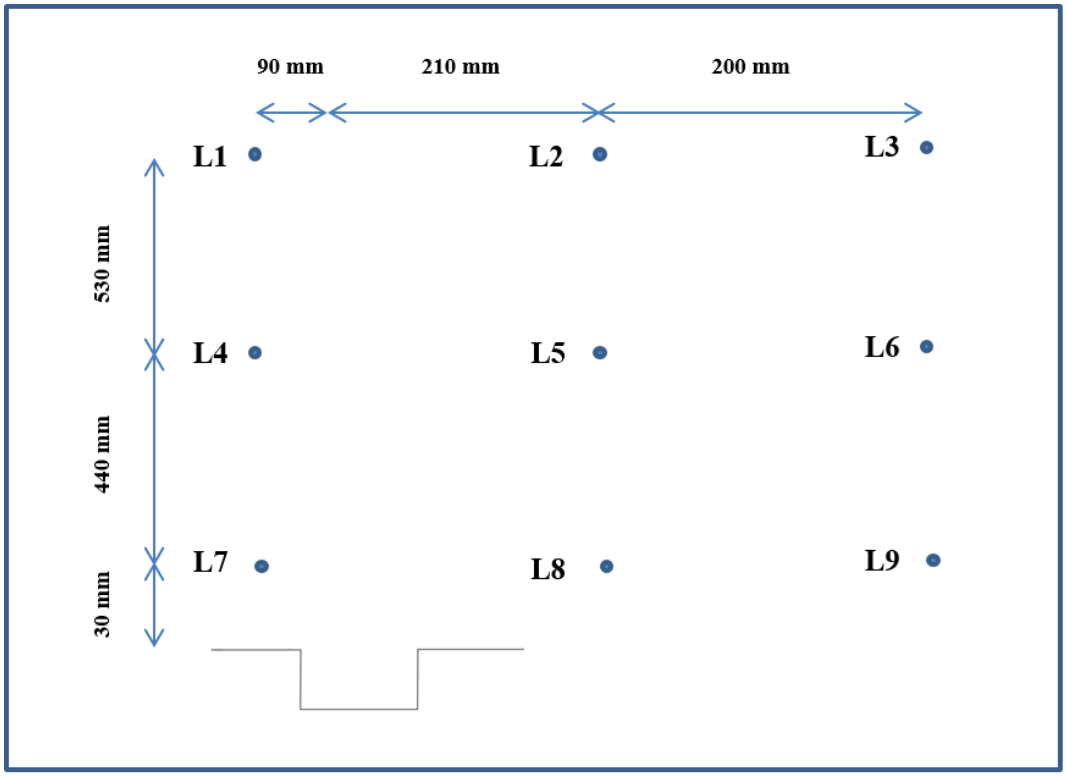

Figure 5.12: Listener positions.

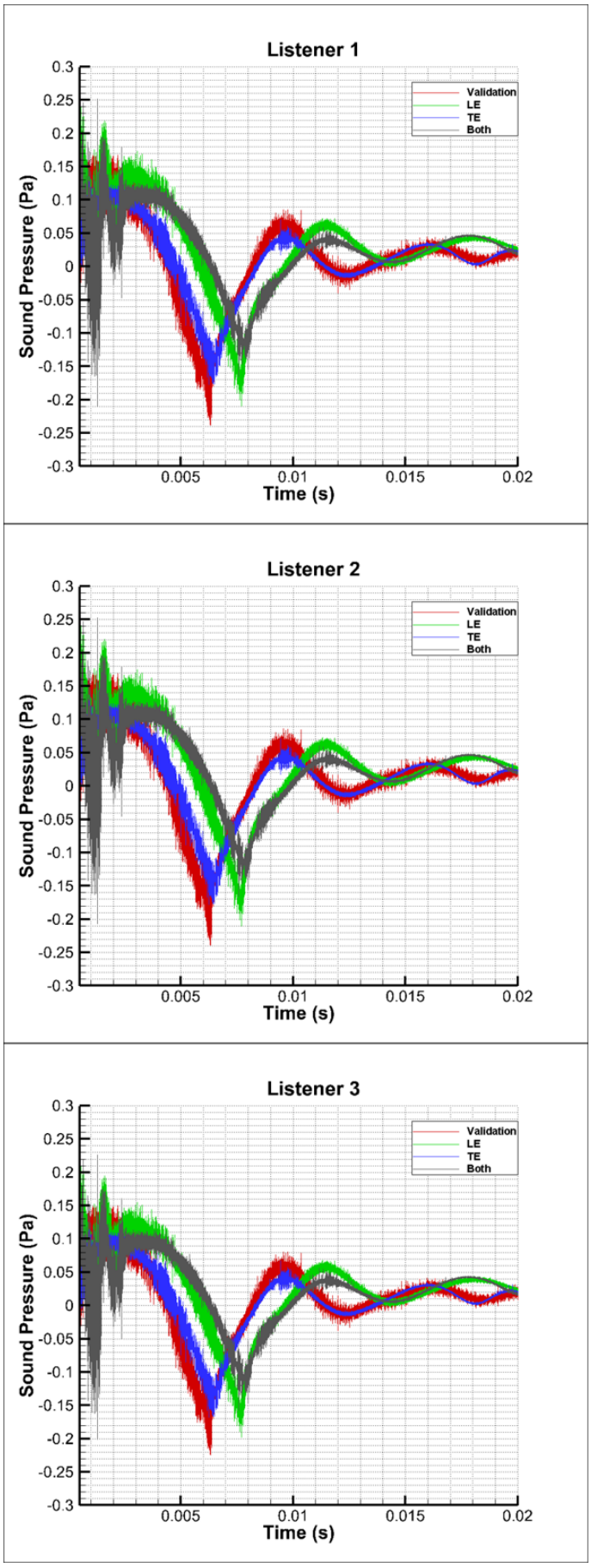

Figure 5.13: Sound pressures at listeners 1,2,3.

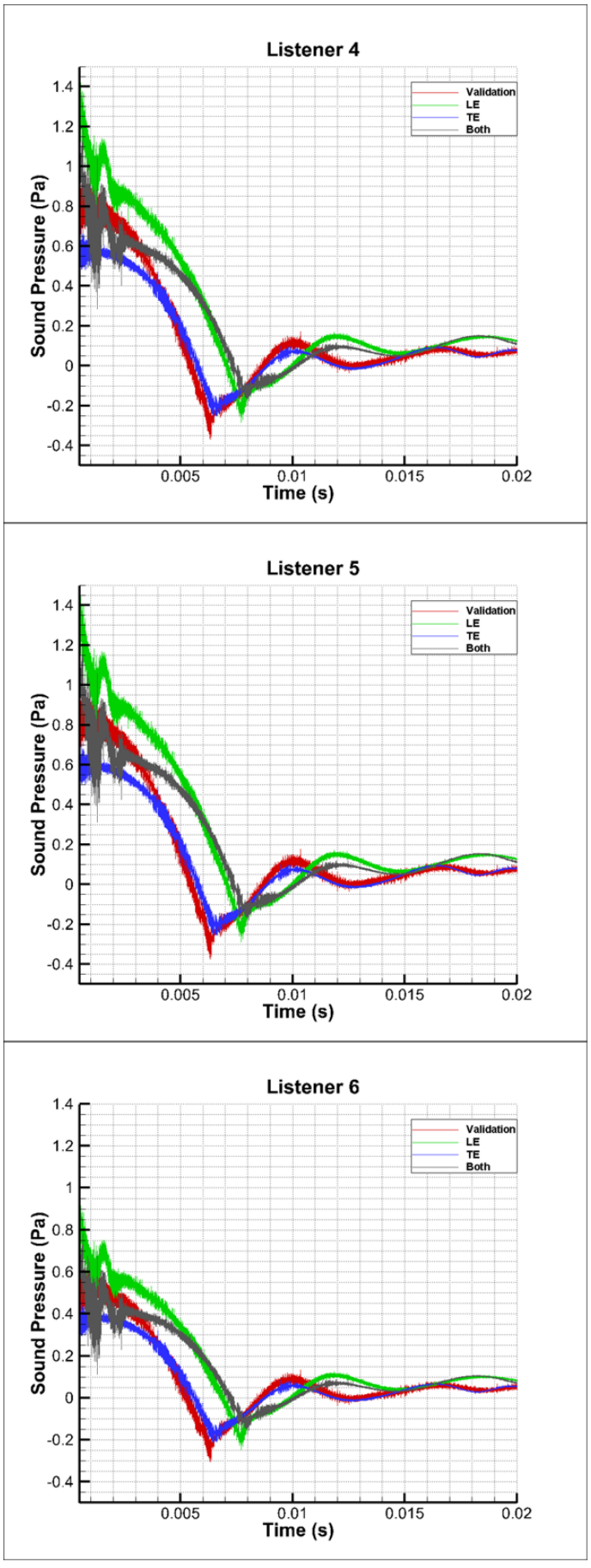

Figure 5.14: Sound pressures at listeners 4,5,6.

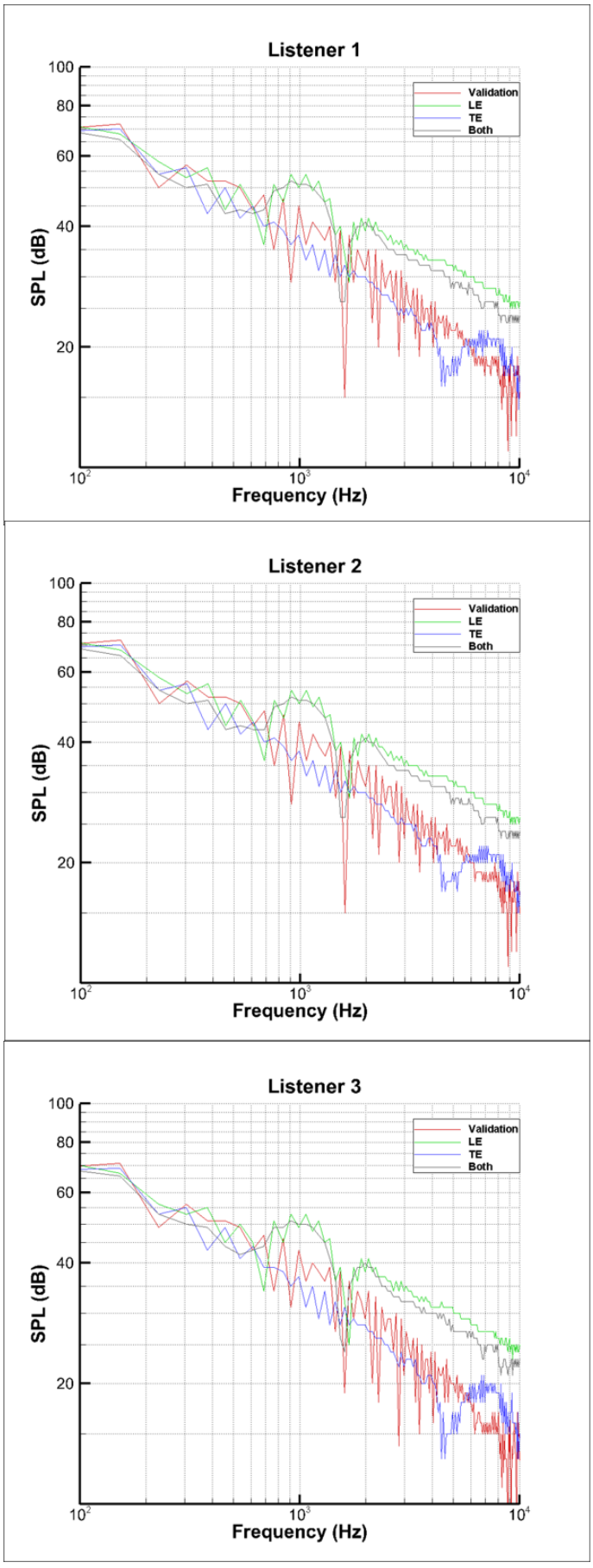

Figure 5.15: Sound pressure levels at listeners 1,2,3.

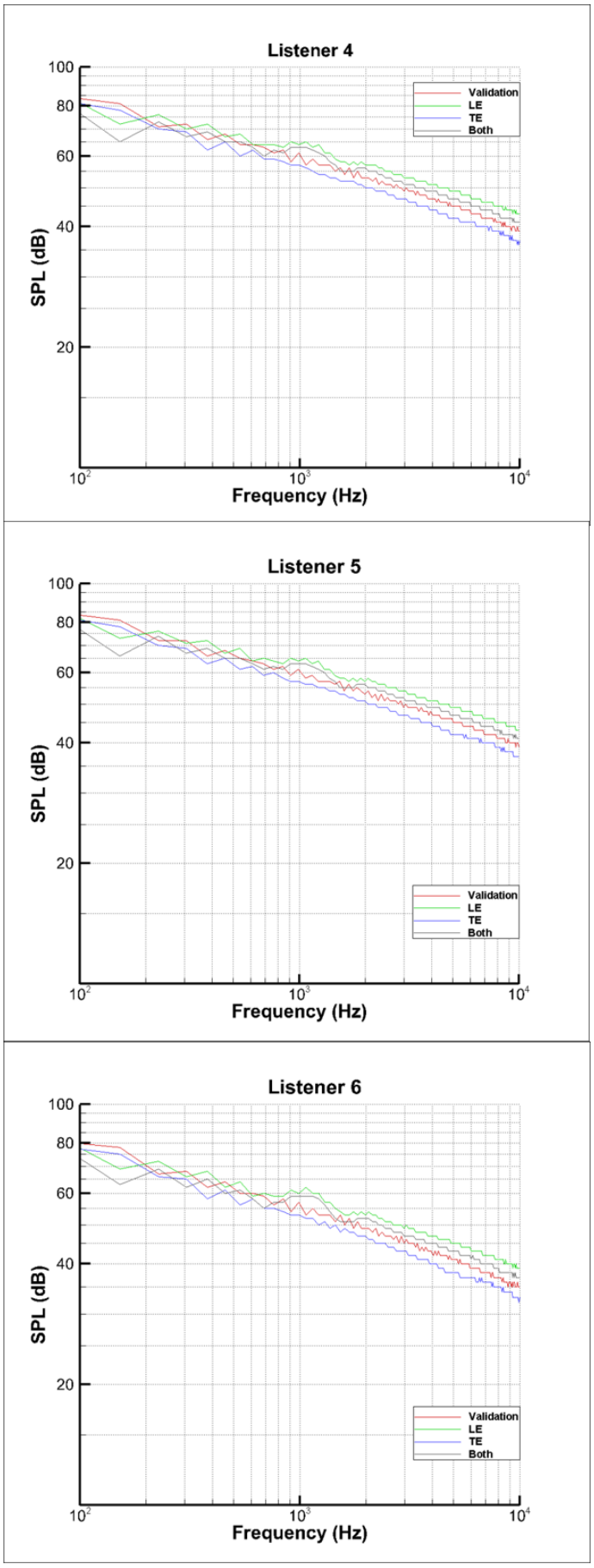

Figure 5.16: Sound pressure levels at listeners 4,5,6.

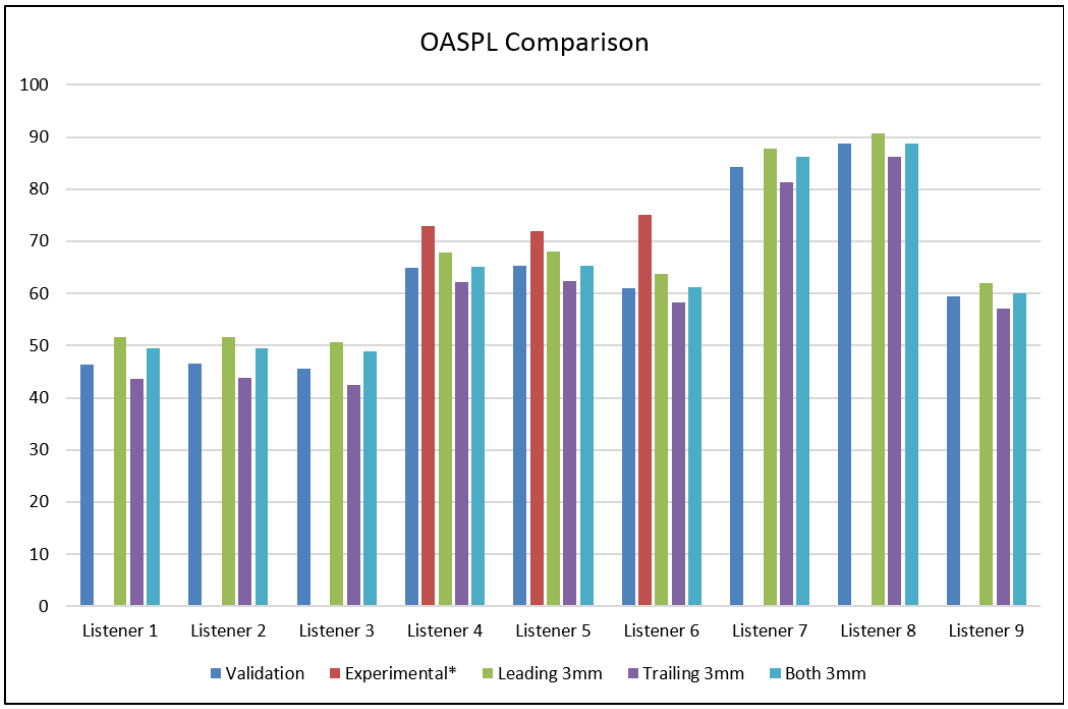

Figure 5.17: Overall averaged sound pressure levels at all listeners.

6. CONCLUSIONS AND RECOMMENDATIONS

The main purpose of this thesis is to develop a home-made program to calculate the sound generated by cavities. To achieve this goal, first the features of the flow is investigated. Important features of the cavity flow are examined. As a part of this, self-sustained oscillations and the characteristics of their types are covered.

After the understanding the flow mechanisms, the method of sound generation calculation is selected. Different computational aeroacoustic methods are investigated and the proper one which is Modified Curle's Analogy is selected.

Computational fluid dynamics anaylses with different geometries are conducted with a commercial CFD tool. Analyses were conducted by using Unsteady Reynolds Averaging Navier-Stokes, Implicit Solver, $k-\varepsilon$ turbulence model and time step of 10^{-7}. Pressure data from the cavity walls are obtained and fed to the home-made program to gather sound datas.

Results are compared with a former experimental work and have close agreement. It is observed that geometry with leading edge rounding has the highest overall sound pressure levels and geometry with trailing edge rounding has the least overall sound pressure levels at all listeners. Also, listeners which are further and has angle further to 90 degrees with sources have higher overall sound pressure levels.

It is important to state that expected peaks at sound pressure level graphics were not seen. For improving this, analyses with different turbulence models should be conducted. Also, a more direct Curle's Equation (with fewer modifications) should be used in further home-made programs. 3D parts of the equations may be implemented in the program too. Also, investigating the Rossiter modes of cavities with different geometries can be a useful study for future works.

REFERENCES

Colonius, T. et al. (1999) "Numerical Investigation of the Flow Past a Cavity," AIAA Paper, pp. 99-1912.

Curle, N. (1955) "The Influence of Solid Boundaries Upon Aerodynamic Sound," Proc. Roy. Soc. London Ser., A 231, pp. 505-514.

Ffowcs Williams, J. E. and Hawkings, D. L. (1969) "Sound Generation by Turbulence and Surfaces in Arbitrary Motion," Philos. Trans. Roy. Soc., A264, pp. 231-342.

Franke, M. E. and Carr, D. L. (1975) "Effect of Geometry on Open Cavity Flow-Induced Pressure Oscillations", AIAA Paper 75-492, AIAA 2nd Aero-Acoustic Conference, Hampton, VA, Mar. 24-26.

Gharib, M. and Roshko, A. (1987) "The Effect of Flow Oscillations On Cavity Drag," Journal of Fluid Mechanic Digital Archive, Vol. 177(-1), pp. 501-530.

Haigermoser, C., Scarano, F., Onorato, M. (2009) "Application of an Acoustic Analogy to PIV Data from Rectangular Cavity Flows," Experiments in Fluids, Vol. 46, pp. 517-526.

Larsson, J., Davidson, L., Eriksson, E. and Olsson, M. (2004) "Aeroacoustic Investigation of an Open Cavity at Low Mach number," AIAA Journal, Vol. 42, pp. 2462-2473.

E. Lazar, G. Elliott, N. Glumac (2008) Control of the Shear Layer Above a Supersonic Cavity Using Energy Deposition, AIAA Journal, 46 2987 2997 .

Ligthill, M. J. (1952) "On Sound Generated Aerodynamically," Proc. Roy. Soc. London Ser., Vol. 211(1107), pp. 564-587.

Maull, D.J. and East, L.F. (1963) "Three-dimensional Flow in Cavities," Journal of Fluid Mechanics Digital Archive, Vol. 16(04), pp. 620-632.

Moon, Y. J., Seo, J.-H., Koh, S.-R., Cho, Y. (2003) "Aeroacoustic Tonal Noise Prediction of Open Cavity Flows Involving Feedback," Computational Mechanics, Vol. 31, pp. 359-366.

Parkhi, D. (2009) "Aeroacoustics of Cavity Flow Using Time-Resolved Particle Image Velocimetry", Master of Science Thesis, Technical University of Delft, Delft, The Netherlands.

Pereira, J.C.F. and Sousa, J.M.M, (1995) "Experimental and Numerical Investigation of Flow Oscillations in Rectangular Cavity", Journal of Fluids Engineering, Vol. 117, pp. 68-74.

Rockwell, D. and Naudascher, E. (1978) "Review – Self-sustaining Oscillations of Flow Past Cavities," ASME Transactions Journal of Fluids Engineering, Vol. 100, pp. 152-165.

Rossiter, J.E. (1964) "Wind-tunnel Experiments on the Flow over Rectangular Cavities at Subsonic and Transonic Speeds," Journal of Fluid Mechanics Digital Archive, (3438).

Sarohia, V. and Massier, P. F. (1977) "Control of Cavity Noise", Journal of Aircraft, Vol. 14, No. 9, pp. 833-837.

Stratton, J. A. (1941) "Electromagnetic Theory," McGraw Hill, New York.

Tam, C. K. W., (1976) "The Acoustic Modes of a Two-dimensional Rectangular Cavity," Journal of Sound Vibration, Vol. 49, pp. 353-364.

CURRICULUM VITAE

Name Surname: Evren Yenigelen

Place and Date of Birth: Kadıköy, 19/10/1991

Adress: Hacımuhtar sok. Gürdamar apt. No:6/33 Kadıköy/İSTANBUL

E-Mail: evrenyenigelen@gmail.com

B.Sc.: Istanbul Technical University, Aeronautical Engineering, July 2013